We are IntechOpen,
the world's leading publisher of
Open Access books
Built by scientists, for scientists

6,100
Open access books available

149,000
International authors and editors

185M
Downloads

154
Countries delivered to

Our authors are among the
TOP 1%
most cited scientists

12.2%
Contributors from top 500 universities

WEB OF SCIENCE™
Selection of our books indexed in the Book Citation Index
in Web of Science™ Core Collection (BKCI)

Interested in publishing with us?
Contact book.department@intechopen.com

Numbers displayed above are based on latest data collected.
For more information visit www.intechopen.com

Chapter

Welding Properties of Titanium Alloys Grade 5

Alireza Farrokhi

Abstract

Titanium alloys have attractive properties that have been widely used in various fields due to these properties. The biocompatibility of titanium has caused its usages in the pharmaceutical industry. Its good corrosion resistance has resulted in its many applications in petrochemical and marine industries. Meanwhile, the most important and major application of titanium and its alloys can be found in the aerospace industry in a variety of spacecraft, space rockets, and satellites. The most important reason for the widespread use of these alloys in the aerospace industry is the high ratio of strength to their weights. However, the most important factor limiting the usage of titanium and its alloys is its high price. In this chapter, we first introduced titanium and its alloys. Then, according to mainstream of the design, titanium alloy bonding methods and welding problems have been investigated. The purpose of this study is to investigate the processes of arc welding of tungsten electrode-neutral gas with different alloy heat inputs for a titanium alloy of Ti-6Al-4 V and to provide comprehensive welding instructions. So, after introducing the pure commercial titanium properties, we examined the properties, specifications and welding of Ti-6Al-4 V. Given the focus on the mentioned process, the generalities of this welding process have been described.

Keywords: procedure qualification record, welding procedure specification, Ti-6 Al-4 V titanium alloy grade 5, gas tungsten inert gas, tungsten inert gas, fusion zone, heat affected zone

1. Introduction

High ratio of strength to weight and the desired properties of corrosion resistance of titanium alloys have provided special applications to these alloys. However, high actual cost of making these alloys has limited their usages. The price of this metal is considerably higher than widely used industrial metals such as steel, copper and aluminum. On the other hand, the speed of the machining of titanium is about 10 to 100 [1, 5] times slower than machining of aluminum and in cases where the speed of production is a priority, the use of titanium is not profitable. One of the problems with welding titanium alloys is formation of a frangible structure. Factors such as type of welding process and the degree of cleanliness of the surface of the components and the degree of protection are effective on forming this defect and other defects of titanium welding. Researches have shown that by changing the essential variables, Ti-6Al-4 V

IntechOpen

is one of the most commonly used alloys of titanium due to its combination of desirable physical and mechanical properties. In order to improve the mechanical properties of this alloy, thermal operation is carried out on it [1, 5]; but during welding these properties change with resizing of grains, the ratio of phases, morphology and microstructure. It should be possible to design processes, by taking into account the appropriate variables that can maintain the desired properties of these alloys and even improve some of them.

In welding of titanium alloys, GTAW or TIG (Gas Tungsten Arc Welding or Tungsten Inert Gas) process is widely used because of the simultaneous provision of high quality at low actual cost. The basis of this method is to create a weld bonding by making electric arc with a non-consumable tungsten electrode and protecting the molten pool through a protective gas stream. In tungsten inert gas welding, the grains are stretched [1, 5]. As a result, mechanical properties such as toughness and ductility are reduced. Due to high activity of this metal, the protection of the weld area is carried out even up to a temperature of 426° C [1, 5]. In the conducted researches, the ultimate tensile strength of the weld area of this alloy has been reported between 925 and 1060 MPa [1, 5]. Also, in comparison to the strength of the weld area and the base material, contradictory results have been reported. That is, both lower strength and greater strength of the weld area than the base material have been reported. This is due to effect of the type of welding process and the thermal operation after welding on the final properties of the weld area. The martensitic microstructure, which is formed in high-energy welding processes, has a higher hardness and strength than the products of this arc welding process. Ductility of weld area is less than the base material. Increase in length of this alloy is 11% in melting mode and 16% in the worked mode. However, this quantity has been reported less than 6% [1, 5] for its weld area. In welding of this alloy the least degree of ductility is achieved in method of tungsten inert gas (TIG) and the most degree of that is achieved by electron beam welding. By performing thermal operation after welding, this low ductility can be increased, though not as much as metal-base ductility. The weld area is strongly affected by the beta phase grain size. So, in some cases, by performing a TIG process using pulse current, the beta grain size can be reduced and thus toughness can be increased. In this alloy, by controlling microstructure the fracture toughness and the resistance to fatigue cracking in better weld area can be usually improved even compared to the base metal, which is achieved through the formation of a fine layer microstructure.

As other welding processes, the properties of the final product of GTAW welding are influenced by variables of this process (such as intensity of welding current, cooling rate, welding rate and protective gas flow, porosity in the weld area also varies). Some of these variables are welding current, voltage, electrode type and diameter, chemical composition and protective gas flow rate, welding rate, and so forth. By changing these variables, the ultimate weld properties can be changed. It should be noted that sum of effects of these variables can be found in the quantitative effectiveness called heat input. In other words, each of these variables can directly or indirectly affect the heat input and thus affect the ultimate property of weld. This quantity represents the amount of energy transferred per weld length unit. Voltage, current and welding rate directly affect this quantity, and parameters such as diameter of electrode by affecting the relative density of the current and the neutral gas flow rate by changing the heat transfer around the weld, indirectly affect this quantity. Excessive heat input can cause problems such as weld cracking and reduction in mechanical properties of the piece.

In this research, after selecting the intended variables and their change levels, welding operation was performed on alloy sheets of Ti-6Al-4 V through GTAW method. In the end, the effect of variables of current intensity and welding voltage on the properties of the final product was investigated by examining the depth of welding penetration, the mechanical properties of the weld, the microstructure and the base metal of the weld area and its surrounding areas. In addition, the cost comparison of manual and automatic welding processes has been put in **Table 1**.

1.1 Purpose of the research

The purpose of this study was to investigate the effect of electric current intensity in the process of arc-welding with tungsten electrode. Due to the fact that titanium metal is widely used in advanced industries such as aerospace and it is also difficult to welding with conventional methods, this material has been used for welding in this study. In this research, the process of welding arc-welding with tungsten electrode (GTAW) was used to weld titanium sheets. Preparation of the welding seam with V shape was carried out, and it was used of the protective gas of the melting pool and the secondary protective gas and back protective gas to provide complete protection

Method of welding	Manual	Automatic
Welding Current (amps)	240	300
Welding Voltage (volts)	25	30
Travel Speed (in/min)	10	15
Gas Flow (f^3/hr)	30	40
Welding Time (hr)	0.057	0.022
Arc Time (hr)	0.02	0.013
Labor + Overhead Cost ($/hr)	18	18
Operator Factor (%)	35	60
Weight of Deposit (lbs)	0.037	0.037
Filler Wire Cost ($/lb)	1.6	1.6
Deposition Efficiency (%)	100	100
Gas Cost ($/$f^3$)	0.06	0.06
Gas Used (f^3)	0.6	0.53
Electric Power Cost ($/kw-hr)	0.035	0.035
Power Source Efficiency (%)	50	50
Labor + Overhead Cost ($/ft)	1.026	0.396
Filler Wire Cost ($/ft)	0.059	0.059
Shielding Gas Cost ($/ft)	0.036	0.032
Electrode Cost ($/ft)	0.001	0.001
Electric Power Cost ($/ft)	0.008	0.008
Total Cost ($/ft)	**1.130**	**0.496**

Table 1.
Cost comparison of manual vs. automatic welding [2].

during the welding. At first, the welding process was performed with three electric current of 80, 90 and 100 amps. Then, PQP samples were prepared according to ASMEM sec IX standard, and tension, impact and hardness tests were performed on them.

2. Review on references

2.1 Titanium and its alloys

The pure titanium has a high coefficient of friction and a low hardness; therefore, it has low wear resistance. The density of titanium is about half of steel. Although titanium has the highest strength-to-weight ratio among highly used industrial metals, but its high price limits its use. Titanium has a strong tendency to react with oxygen. High corrosion resistance of this alloy is due to formation of a sticky oxide layer at its surface. Incompleteness of the last titanium electron layer has caused the element to form solid solvent by creating ionic and covalent bonds with many elements. Titanium alloys are used in the aerospace, chemical and medical industries due to their corrosion resistance, high strength-to-weight ratio and maintenance of strength at high temperatures [1, 5]. **Table 2** shows the important properties of titanium with other metals widely used in the industry.

Titanium is transformed from phase α which has HCP structure to phase β with BCC structure at 882° C. The phase transformation makes the possibility of creating different thermal operations for obtaining various microstructures. Schematic description of titanium phases and their main transformation temperatures are shown in **Figure 1**.

The classification of titanium alloy elements is based on their effect on the phase transformation of α to β. The temperature of this phase transformation depends on the type and amount of elements in titanium alloys. From this perspective, these elements are divided into three groups of neutral, phase stabilizer α and phase stabilizer β. This division is presented in **Table 3**.

	Ti	Fe	Ni	Al	Cu
Melting point (C °)	1670	1538	1455	660	1084
Phase transformation	α to β	α to γ	—	—	α to β
Phase transformation temperature (C °)	882	912	—	—	810
Crystal structure	BCC، HCP	FCC، BCC	FCC	FCC	FCC
Elastic Modulus (GPa)	115	215	200	72	125
Degree of yield strength (MPa)	1000	1000	1000	500	1000
Density (g / cm^3)	4.5	7.9	8.9	2.7	8.94
Corrosion resistance	Very high	Low	Medium	High	High
Reactivity with oxygen	Very high	Low	Low	High	Low
Relative price	Very high	Low	High	Medium	Medium

Table 2.
Comparing properties of titanium with other important industrial metals [4].

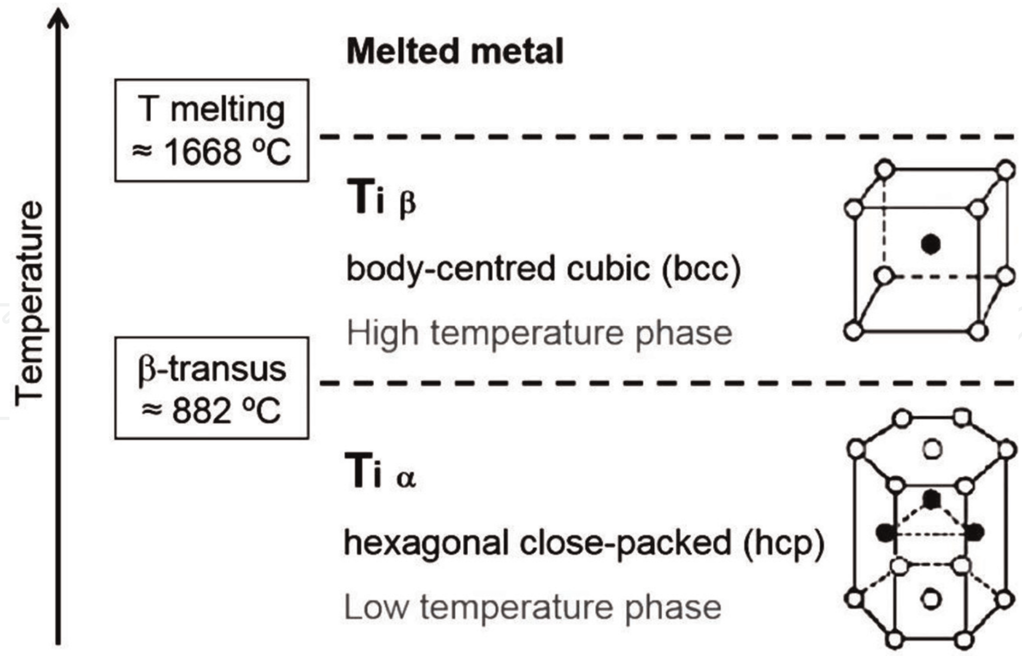

Figure 1.
Schematic description of titanium phases and main transformation temperatures [5].

Type of element	Name of element
Neutral	Tin, zirconium
phase stabilizer α	Aluminum, carbon, nitrogen, oxygen, germanium
β Isomorph	Molybdenum, Vanadium, Tantalum, Niobium
β Eutectoid	Iron, manganese, chromium, cobalt, nickel, copper, silicon, hydrogen

Table 3.
Classification of titanium alloy elements [1].

Neutral elements do not have much effect on this transformation; while phase-stabilizing elements of α stabilize phase α to higher temperatures than transformation temperature, and phase-stabilizing elements of phase β cause the phase to be stable at lower temperatures than transformation. Stabilizers of phase α, in addition to stabilizing this phase, also expand two-phase area of α + β at higher temperatures than the transformation temperature. Stabilizers of phase β are divided into two categories. The first group creates a two-part isomorphic system with a relatively good solubility. The other group creates a eutectoid point in the phase diagram and forms intermetallic compounds [1, 3, 7]. Phase diagrams of titanium based on the type of alloying elements are shown in **Figure 2**.

Titanium alloys, in terms of microstructure, are divided into three main groups of α, β and α + β, and two subgroups of close to α and close to β (pseudo-β). Alloys containing stabilizing elements of phase α and neutral elements are included in α alloys. By adding small amounts of β-phase stabilizers to α alloys, α alloys are formed, and subsequently the phase mixture of α + β alloy is formed, by increasing the stabilizing elements of β, if the amount of these elements is sufficiently large, phase β is formed lonely, and if it is not enough to make martensitic phase by quenching the alloy, it is called pseudo-β alloy. α alloys have low relative strength compared to β, but their properties are well maintained at high temperatures. Shaping of two-phase α + β

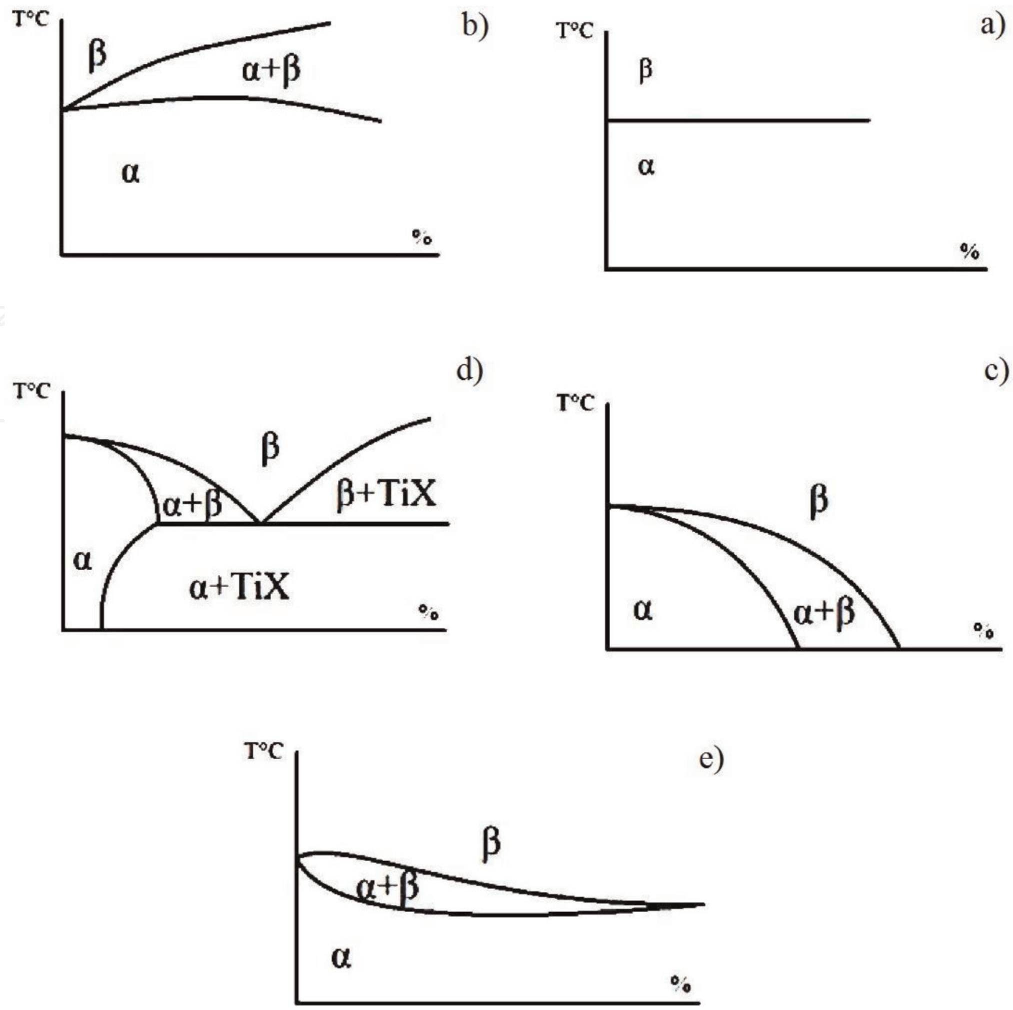

Figure 2.
Phase diagrams of titanium based on the type of alloying elements; a) pure titanium, b) stabilizer α, c) isomorph β, d) β-eutectic, e) neutral [6].

alloys is more convenient than α alloys, but it is more difficult than β alloys [6–8]. **Table 4** shows the important commercial titanium alloys of α and α + β, and **Figure 3** shows the phase stability diagram of titanium alloys based on concentration of stabilizing alloying elements of phase β.

2.2 Bonding of titanium and its alloys

One of the most important methods for bonding these alloys is fusion welding, non-fusion welding, such as friction welding and hard soldering. Due to very high activity of titanium, its bonding processes should be carried out under specific conditions, so that the molten pool and also solid titanium are protected well. For fusion welding of titanium alloys, five main methods are used including arc welding with tungsten electrode (non-consumable electrode), arc welding with metal electrode (consumable electrode), electron beam welding, plasma arc welding and laser welding; among these methods, TIG method is more common [10–15]. Of course, in each of these melting methods, there is the risk of contamination of the alloy by elements such as oxygen, nitrogen, and hydrogen. On the other hand, the production of suitable fillers for titanium alloy titanium welding has problems. First, it is very hard to produce wire of titanium alloys, which has both high strength and relatively low ductility. Secondly, in the case of producing these wires, the actual cost is too

Common name	Alloy composition (wt %)	$_{\beta}$T (C)°
	α alloys and commercial pure titanium	
Grade 1	CP-Ti (0.2Fe, 0.18O)	890
Grade 2	CP-Ti (0.3Fe, 0.25O)	915
Grade 3	CP-Ti (0.3Fe, 0.35O)	920
Grade 4	CP-Ti (0.5Fe, 0.40O)	950
Grade 7	Ti-0.2Pd	915
Grade 12	Ti-0.3Mo-0.8Ni	880
Ti-5-2.5	Ti-5Al-2.5Sn	1040
Ti-3-2.5	Ti-3Al-2.5 V	935
	α + β alloys	
Ti-811	Ti-8Al-1 V-1Mo	1040
IMI 685	Ti-6Al-5Zr-0.5Mo-0.25Si	1020
IMI 834	Ti-5.8Al-4Sn-3.5Zr-0.5Mo-0.7Nb-0.35Si-0.06C	1045
Ti-6242	Ti-6Al-2Sn-4Zr-2Mo-0.1Si	995
Ti-6-4	Ti-6Al-4 V (0.20O)	995
Ti-6-4 ELI	Ti-6Al-4 V (0.13O)	975
Ti-662	Ti-6Al-6 V-2Sn	945
IMI 550	Ti-4Al-2Sn-4Mo-0.5Si	975

Table 4.
Important commercial titanium alloys of α and α + β [3].

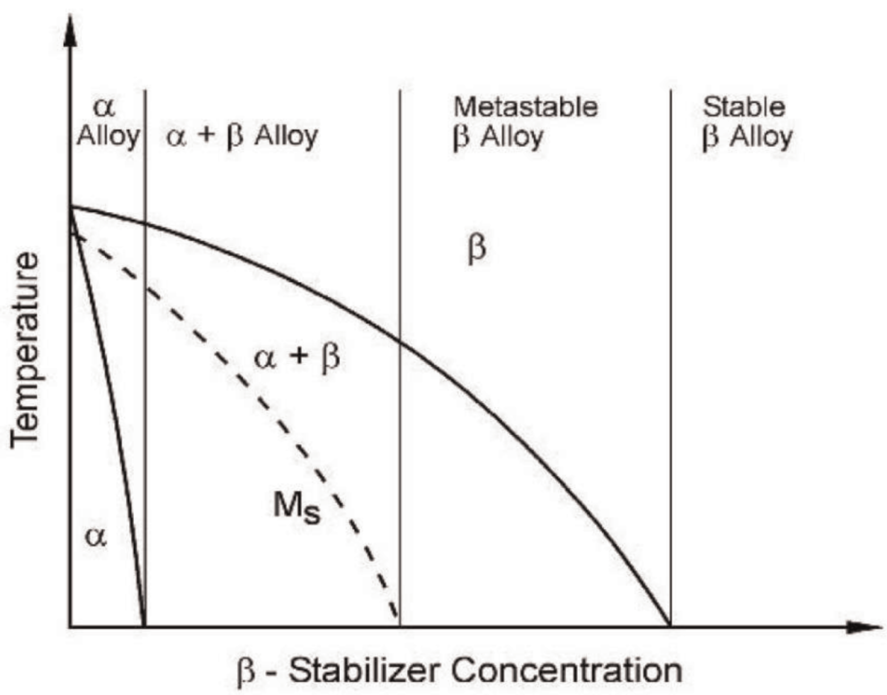

Figure 3.
Phase stability diagram of titanium alloys based on concentration of stabilizing alloying elements of phase β [3].

high. MIG (consumable electrode) method is used when the welding seam is large and the filler wire is selected homogeneous with the consumable electrode. Plasma arc welding was proposed as an alternative to TIG method. The area affected by heat in this method is narrower than the same area of the TIG method. In this method, the thermal source for metal melting is plasma torch [15–18]. The specifications of the four methods for fusion welding of titanium alloys are shown in **Figure 4**. According to the figure, in methods based on high-energy beams such as laser method (LBW) and electron beam method (EBW), the weld area is deeper and narrower than the arc method. In addition, their heat input is less than arc method. This less heat is equal to residual stresses and less distortion in the workpiece.

For successful welding of titanium alloys, it should be noted that titanium is highly active and reactive, especially at temperatures above 500. This material can react with elements in impurities or air such as carbon, oxygen, nitrogen, and hydrogen. Although these elements can increase titanium strength under certain conditions, but they can reduce the ductility and tensile strength of titanium connections. On the other hand, along with high reactivity of titanium, effects of heating and cooling cycles that affect mechanical properties and chemical composition of titanium connections during welding processes also need to be considered [8, 21].

TIG process can be done either manually or automatically, and the heat source and welded wire can be independently controlled. The process can be done depending on the conditions, either using a welded wire or without it. The connections created by TIG method usually have high quality and the amount of defects, splashing (spatter) and slag is low, which is why cleaning after welding is usually not considered a key step. One of the other advantages of this method is the relatively inexpensive equipment of that. On the other hand, the welding rate in this method and the sedimentation rate are low, which is why this method is not efficient for welding thick parts. This process is sensitive to the contamination in the weld wire and the base metal, and the magnetic field causes deviation of the arc. All of these factors make controlling the process difficult. Also, the heat input is very high [22–24].

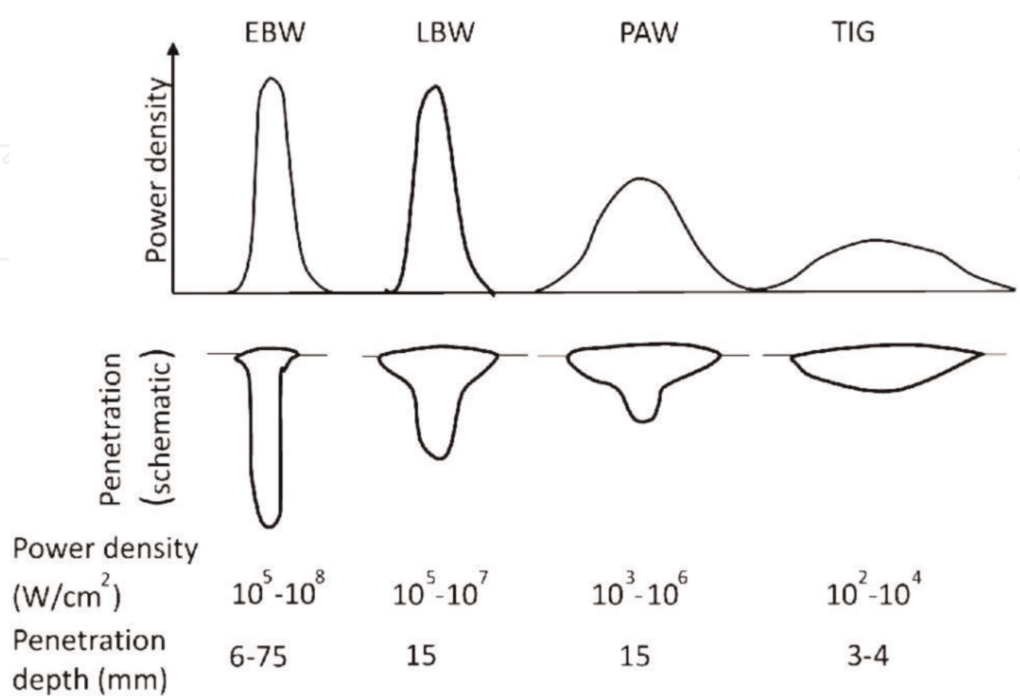

Figure 4.
Comparing specifications of welded titanium specimens by fusion methods [20].

2.3 Problems with welding of titanium alloys

Welding of titanium and its alloys has some problems. Some of these problems include:

- Preventing the mixing of the molten at the weld edge due to formation of oxides,
- Cracks,
- Creation of porosity
- Presence of oxides in the form of offal in the weld metal,
- Although dissolution of oxygen and nitrogen in titanium increases its hardness, but dissolution of hydrogen causes loss of toughness and increase of sensitivity to crack of the alloy.
- Formation of highly stable carbides in the event of reaction wit carbon at high temperatures; although in some cases, small amounts of carbon are added to this alloy to obtain the alloy with high hardness and strength, but in general it can be said that formation of these carbide phases makes the alloy frangibility [25–27].

2.4 Ti-6Al-4 V

Toughness of the two-phase $\alpha + \beta$ alloys is high. An optimal combination of toughness and fatigue strength in these alloys is created by thermo mechanical operation. The most important alloy of this group is Ti-6Al-4 V or IMI 318. The alloy, used in the manufacture of jet engine fan blades, accounts for more than half of sales of titanium alloys, and the alloy is used in more than 80 percent of applications related to aerospace of titanium alloys. In cases where high corrosion resistance is considered along with high strength and toughness, this alloy is used. In this alloy, aluminum and vanadium are respectively, stabilizers of phase α and β. In the industry, this alloy exists as two grades of 23 or ELI and Grade 5. The chemical composition of this alloy is shown in **Table 5** and its physical and mechanical properties are given in **Table 6**.

Due to formation of hard and needle-like phase of martensite and large grain size of phase β in the penetrative area, which reduces its ductility, this alloy does not have much suitable capability of weldability. Generally, to improve the properties of the weld area, the grain size of phase β is tried to be decreased and the amount of heat input is also controlled at an optimum size. Comparison of the tensile strength of this material at various temperatures with other materials is shown in **Figure 5**. As it can be seen, in the range of working temperature of 400–500° C, this alloy has the highest specific strength among different materials [12, 27, 29, 30].

Name of element	Al	V	Fe	O	N	C	H	Other impurities	Total other impurities
Min wt%	5.5	5.3	—	—	—	—	—	—	—
Max wt%	6.75	4.5	0.3	0.2	0.03	0.08	0.125	0.1	0.4

Table 5.
Chemical composition of Ti-6Al-4 V [8].

Property	Value
Density	g/cm^3 4.43
Melting point (°C)	1604–1660
Elastic modulus	GPa1113.8
Thermal conductivity	W/m.K 6.7
Electrical resistance	0.000178 Ohm-centimeters
Thermal expansion	/K8.9*10–6
Tensile strength	MPa 880
Compressive strength	MPa 970
Vickers Hardness	334

Table 6.
Physical and mechanical properties of Ti-6Al-4 V [28].

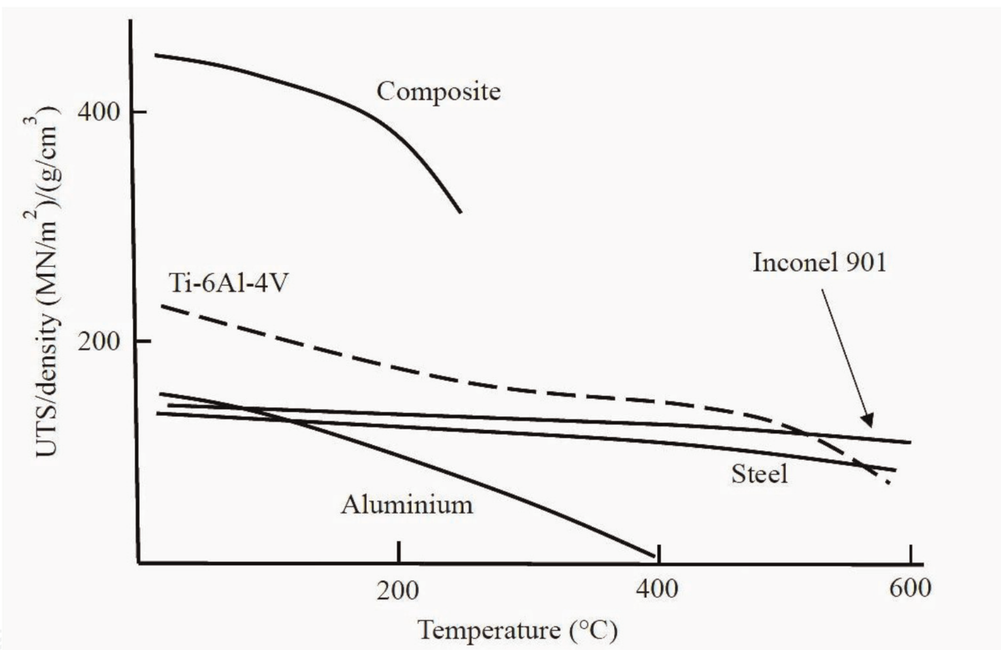

Figure 5.
Comparison of the tensile strength of Ti-6Al-4 V with other materials at various temperatures [20].

2.5 Manual electrode arc welding and protective gas

2.5.1 History of tungsten arc welding

After the discovery of short arc in 1800 and continuous electric arc in 1802, electric arc welding was slowly developed. The idea of welding in inert gas was introduced in 1890. But even in the early 20th century, welding of non-ferrous materials, such as aluminum and magnesium, was still difficult. Because these metals react quickly with air and thus are oxidized and strength of the metal is reduced. The process of using flux as an electrode coating was also not satisfactory and did not protect against contamination. To solve this problem, in 1930, inert gases were used. A few years later, welding under protective gas was used for the first time in aviation industry for welding of magnesium, and in this operation the electric arc formation method was utilized using helium and argon as protective gases and favorable results were obtained [23, 31].

2.5.2 Arc welding with tungsten electrode and inert gas

It is a type of fusion welding which is classified according to DIN 1910 into two general types of TIG welding and arc welding with protective gas or GMAW. The equipment used in the TIG procedure is much cheaper than other methods. This method can be used to weld pieces with thicknesses of 2 to 20 mm with proper efficiency. This method usually uses a current between 50 and 500 amps and a voltage between 10 and 15 volts. The type of electrode is determined according to the desired properties and its diameter is determined proportional to the thickness of the piece and the welding condition. The schematic of TIG welding process is shown in **Figure 6**.

In TIG welding, also known as GTAW, non-consumable tungsten electrode is used which is protected by gas or a mixture of gases. This electrode can be pure tungsten. To increase the arc stability and make it easier to start the arc, a tungsten electrode containing small amounts of oxides such as zirconium oxide, thorium oxide, etc. can be used [14, 15, 21, 32–34]. Specifications of tungsten electrodes are given in **Table 7**.

The sedimentation rate in TIG method is low. This sediment rate can be improved using preheated filler. Due to the fact that the electrode in TIG method is non-consumable, therefore, depending on the thickness of the workpiece, type of connection and ... filler metal also can be used for welding (filler or weld wire). These fillers can be added manually or mechanically to the weld area [20, 35]. Application fillers for TIG welding of titanium and its alloys are listed in **Table 8**. This classification is made by the American Welding Society (AWS).

The created arc contains a plasma environment that provides the required energy to melt the base metal and filler. This plasma environment is created through an electrical discharge between the electrode and the work piece. To create such a good discharge, a high-frequency and about few MHz ignition system is used. The temperature of the arc above the boiling pond area is between 1200 and 1500 Kelvin and at the molten surface it is between 1700 and 2500 Kelvin [37–39].

Although GTAW welding method has advantages over other methods, but compared to other welding methods, the following disadvantages can be noted:

- Lower welding rate than some methods,
- Lower metallurgical quality of the resulted weld than some methods,
- High heat input, which leads to large distortion and the area under the influence of the heat gets bigger,
- Sensitivity to changes in arc length [10–12].

2.5.3 Polarity of welding

In this method, electrical energy is transmitted from the welding torch to the base metal by electric arc. This kind of welding process can be divided into three categories in terms of the used current:

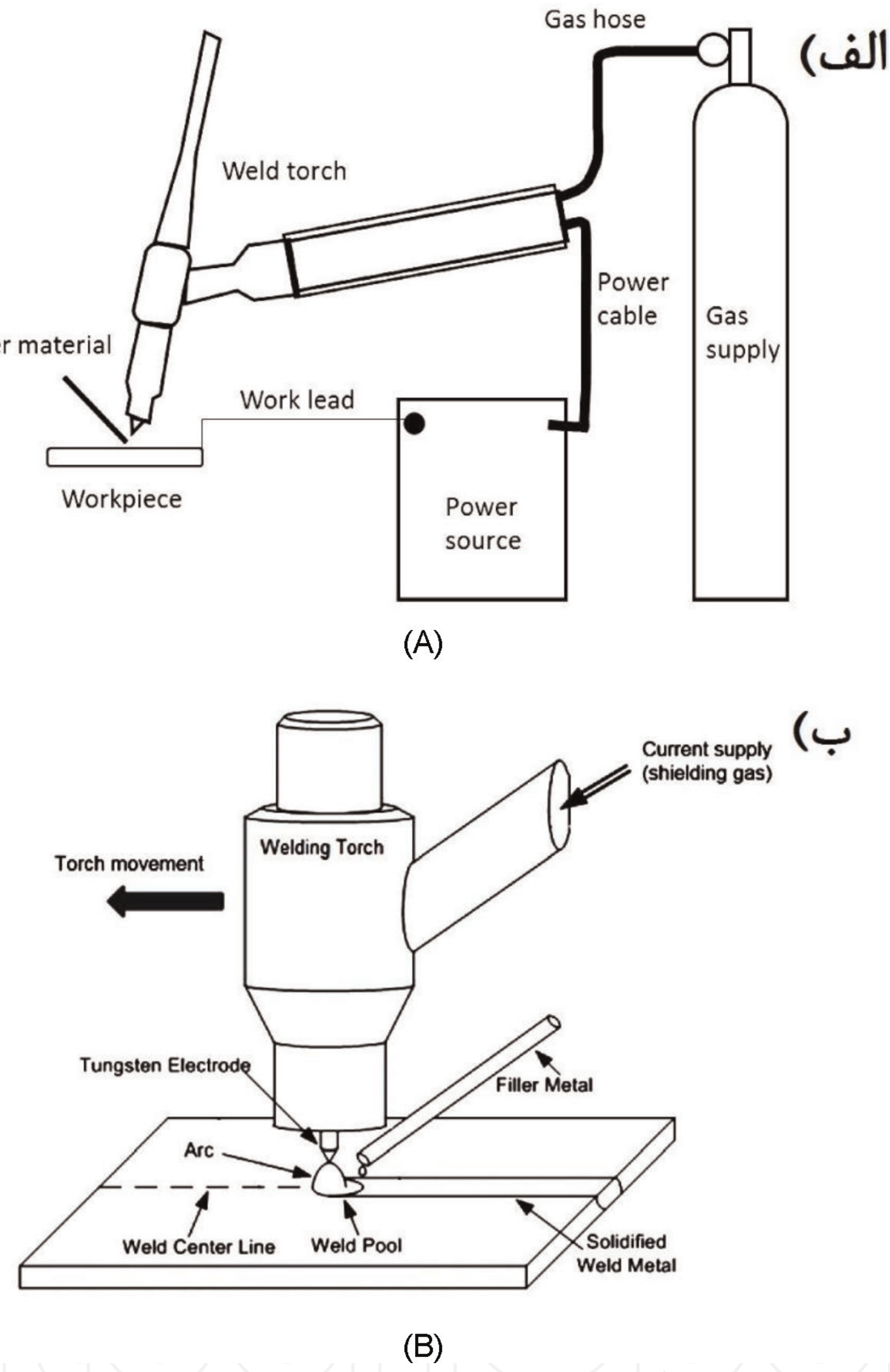

Figure 6.
Process of GTAW; A) schematic of the system used in the process, B) welding principles [6, 20].

- DC Current - Negative-Pole Electrode: This is also called direct polarity mode and is very common in GTAW process. The electrode is connected to the negative pole of the power source. The electrons are emitted from the tungsten electrodes and accelerated passing through the electric arc.

- DC Current - Positive-Pole Electrode: This mode is called Reverse Polarity. The electrode is connected to the positive pole of the power supply. In this situation, the thermal effect of electrons in tungsten electrode is greater than the work piece. Because electron bombardment is toward the electrode. Therefore, an electrode with a large diameter and an anhydrous system is required to be prevented the melting of the tip of the electrode. Positive ions bombard the surface of the work piece, which causes the oxide shells to break down on the work piece. Therefore, this can be used to weld materials with hardened oxide layers such as aluminum and magnesium.

- AC Current: In this case, the penetration and cleaning of the work surfaces of the oxide layers are done well. This is often used for aluminum welding.

Figure 7 shows the effect of polarization systems used in TIG welding processes on the shape of the weld area.

Two other types of currents are pulsed and non-pulsed currents. If there is a need for a very high penetration, pulsed current is used. Direct polarity is the most commonly used polarity in GTAW processes. Through this polarity, high heat in the work piece and, as a result, a high penetration and narrow weld area can be achieved. By choosing alternative current, a combination of cleaning of oxidation from the surface and the proper penetration can be achieved. In TIG welding of titanium alloys, arcs with direct current and tungsten non-consumable electrode as negative pole are

Grouping	Color	Alloying element	Alloy oxide	Nominal weight percent of alloy oxide
EWP	Green	—	—	—
EWCe-2	Orange	Serum	CeO2	2
EWLa-1	Black	Lanthanum	La2O3	1
EWLa1.5	Golden	Lanthanum	La2O3	1.5
EWLa-2	Blue	Lanthanum	La2O3	2
EWTh-1	Yellow	Thorium	ThO2	1
EWTh-2	Red	Thorium	ThO2	2
EWZr-1	Brown	Zirconium	ZrO2	0.25

Table 7.
Tungsten electrodes and tungsten alloys [35].

Weight percent element	ERTi-1	ERTi-2	ERTi-3	ERTi-5	ERTi-7
Nitrogen	0.015	0.020	0.020	0.030	0.020
Carbon	0.03	0.03	0.03	0.05	0.03
Hydrogen	0.005	0.008	0.008	0.015	0.008
Iron	0.10	0.20	0.20	0.22	0.20
Oxygen	0.10	0.10	0.10–0.15	0.12–0.20	0.10
Palladium	—	—	—	—	0.12–0.25
Aluminum	—	—	—	5.5–6.75	—
Vanadium	—	—	—	3.5–4.5	—
Titanium	Rest	Rest	Rest	Rest	Rest
Base material of ASTM	Gr. 1	Gr. 2	Gr. 3	Gr. 5	Gr. 7

Table 8.
Fillers used in welding of titanium alloys [36].

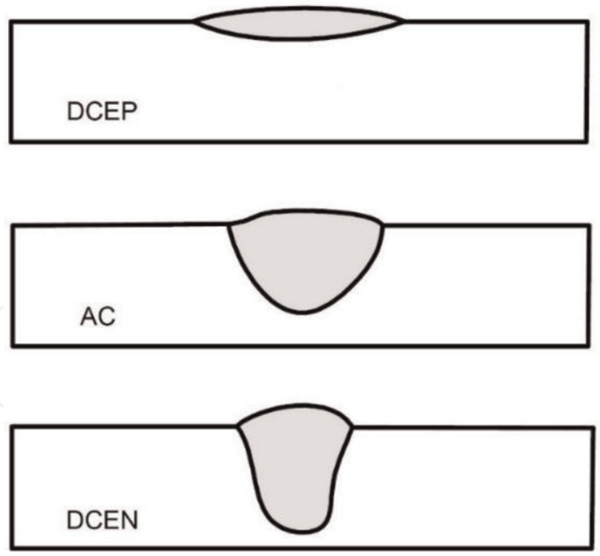

Figure 7.
Effect of current type and polarity on the shape of the weld area [40].

usually used. It should be noted that if there is surplus current, tungsten electrode welding is melted and the tungsten offal will remain in the weld area [11, 15, 23].

2.5.4 Inert gas

The purpose of using inert gas is to create a stable arch, to protect the molten pool and tungsten electrodes against environmental contamination. Some of these gases are argon, helium and their mixture. In welding of major materials, argon is used. Since adding helium to argon improves heat transfer, in welding thick pieces the mixture of these two gases are used. Since argon has low ionization voltage and it is ionized easily, provides this possibility for the arc to be easily arranged and remain stable; therefore it is suitable for working with AC current. Also, argon makes start of arc in AC current easier. Argon generates a column of concentrated arc, and has less capability of thermal conductivity than other gases. Since argon causes stabilization (keeping the arc fixed), it is used in most of mixture of protective gases. The mixture of argon and helium is also used in TIG process when both high penetration and slow arc is considered. The density of argon is approximately same with air, so the same amount of gas that enters the system makes the coating, but the density of helium is one tenth of the air. Therefore, argon should be entered the system 4–5 times more to create the same amount of protective coating. The first ionization energy of helium is extremely high, so the temperature needs to be raised to a large extent. This causes the created arc to be very hot compared to argon. The thermal conductivity of helium is much more than argon; therefore, using helium, the created heat in the center of the arc moves easily and creates a bowl-like area (more open pool). Helium is typically used in industrial processes and argon is used in TIG manual welding. Argon is also much cheaper than helium [3, 23, 41, 42]. Effect of the protective gas composition on the weld geometry and properties of protective gases used in TIG welding are respectively shown in **Figure 8** and **Table 9**.

2.5.5 Heat input

Heat input is a relative quantity that expresses the amount of energy transmitted per length unit of weld. This quantity is directly affected by the mechanical properties

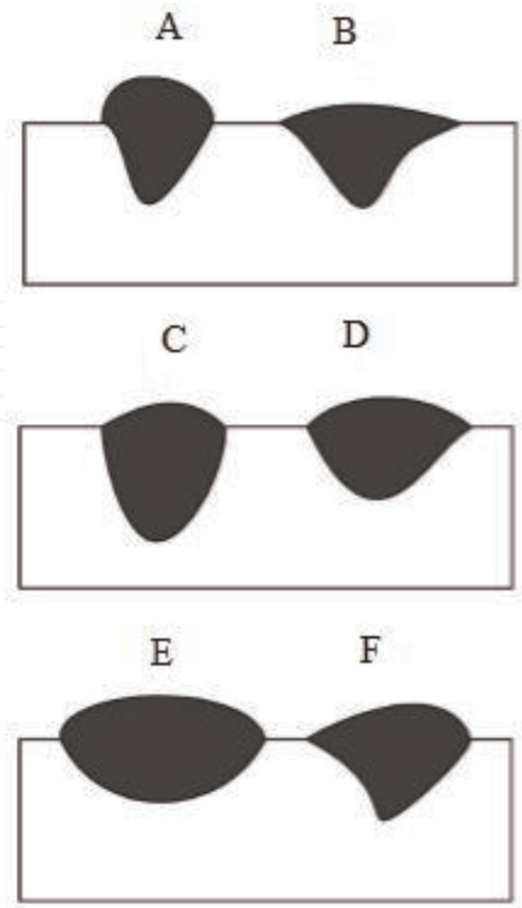

Figure 8.
Effect of the protective gas composition on the geometry of the weld; A) argon; B) mixture of argon and oxygen; C) carbon dioxide, D) mixture of argon and carbon dioxide, E) helium, F) mixture of argon and helium [40].

Gas	Chemical Symbol	Molecular Weight (g/mol)	Specific Gravity of Air	Density (g/L)	Ionization Potential (eV)
Argon	Ar	39.95	1.38	1.784	15.7
carbon dioxide	CO_2	44.01	1.53	1.978	14.1
Helium	H_e	4.00	0.1368	0.178	24.5
Hydrogen	H_2	2.016	0.0695	0.090	13.5
Nitrogen	N_2	28.01	0.967	1.25	14.5
Oxygen	O_2	32.00	1.105	1.43	13.2

Table 9.
Properties of protective gases used in TIG welding [25, 37].

and metallurgical structure of the weld area and the area affected by heat. The following equation is used to calculate the input heat:

$$H = \frac{60\ EI}{1000\ S}$$

where its variables include H: heat input based on Kj/in or kj/mm, E: arc voltage based on volt, I: current based on ampere and S: speed of movement based on in/min or mm/min.

TIG method has a large amount of heat input during welding, and the product of this welding has a large grain size. However, methods such as laser and electron beam welding have fewer heat input than TIG method, and thus reduce the size of the β-phase grain. But these methods have high cooling rates after welding, which increase the amount of needle-shaped martensitic phase. The cooling rate of weld is dependent on the input heat. In Ti-6Al-4 V, phases and various microstructures can be created under different cooling rates, these microstructures determine the final properties of the weld. Therefore, when using these methods, after performing the welding, appropriate heat operation is needed to enhance the ductility of the penetrative area of weld and the area affected by heat. Of course, reducing the amount of input heat is desired to the extent that it does not interrupt the penetration value [39, 43, 44].

2.6 Welding and mechanical properties of Ti-6Al-4 V

The most common method of welding this alloy is TIG, and is usually used for welding the narrow piece of this alloy. For entire-layer microstructures of titanium alloys, beta size parameters, size of alpha colony, width of alpha plates and the presence of grain boundary alpha layer are key microstructural parameters. Among these parameters, the size of the alpha colony, which determines the effective length of slip, is more important. By decreasing the size of alpha colony, yield strength, ductility, microscopic crack germination, and crack propagation resistance increase, while macroscopic crack propagation and fracture toughness increase with increasing size of alpha colony. If martensitic microstructure is formed and a slip length equal to the width of an alpha plate is created, the yield strength is significantly increased [4].

The tensile ductility of entire-layer structure is less than the dual structure. Microcavities can germinate in the alpha-beta intersection due to high dimension ratio of the alpha plates. The number of these intersections is high in entire-layer microstructures.

Reducing the initial beta size has a positive effect on tensile ductility. If the difference between strength among grain boundary alpha layer and transgranular microstructure is high, cracks can germinate in grain boundary alpha layer and lead to intergranular fracture [4, 12].

For a welded area, a fine layer microstructure formed in the melting area and the area affected by heat, has higher hardness than the base metal. The final tensile strength of the titanium alloy weld area has been reported between 925 and 1060 MPa. Based on the carried out researches, the weld area can have a greater or lesser strength than the base metal, depending on the type of welding process and thermal operation treatment welding. Of course, the martensitic microstructure formed in processes with a high energy intensity has higher hardness and strength than the weld created by arc welding methods [9, 45]. Ductility of the weld area can be improved by thermal operation. However, its amount cannot be increased as much as the base metal. Ductility can also be improved by reducing the initial beta grain size. One way to reduce the initial beta grain size is to use pulse current in TIG welding, which can lead to increase in ductility [9, 44–47]. In the weld area, due to formation of fine layer microstructure, fracture toughness and growth resistance of fatigue cracks are greater than the base metal [48].

2.7 Welding parameters affecting weld properties

A part of the weld defects can be eliminated by selecting the right amount of welding variables. In addition, given that the input heat amount is strongly effective on metallurgical properties of the weld, and considering the close direct or indirect bonding of variables of welding and heat input, these are in fact the welding variables that affect the metallurgical properties of the weld.. These properties determine the mechanical properties, corrosion and etc. of a piece. As a result, changing the variables can change the mechanical properties of the weld [27, 49, 50].

As already mentioned, the effect of changing the parameters of the welding process should be sought in how they affect the heat input quantity. Changing the diameter of the electrode changes the density of current, melting rate, sedimentation rate and penetration depth. The lower the diameter of the electrode, the higher the current density and as a result the higher the heat input. On the other hand, in terms of the operation and apparent quality of weld, electrodes with higher diameter, by reducing arc instability, reduce the amount of discharge and result in a cleaner work piece [16]. The change in voltage is strongly effective on the width of the weld area. The voltage also affects the heat input. The higher the welding voltage, the higher the heat input [51]. It is predicted that as the current intensity increases, the penetration depth of the weld will increase due to increase in force on the molten drops. It should be kept in mind that the diameter of the electrode should also be considered in choosing the intensity of the welding current. Because as the electrode diameter is higher, the current intensity must be increased to maintain the current density [52]. In various studies, various inert gases have been used to protect the molten area of GTAW welding of steels. In some researches, effect of mixture of inert gases has been investigated. Inert gases, in addition to the main task which is protection, also affect the heat and heat transfer in the protection zone. By changing the chemical composition of inert gases, the protection level varies. Meanwhile, due to the fact that gases have different heat transfer coefficients, by changing the composition, the amount of heat transferred by the protective gas changes. On the other hand, the change in the rate of the protective gas by affecting the amount of heat transferred by the gas is effective on the amount of heat accumulated in the weld area. It should not be forgotten that, since protective gas is one of the bases of GTAW welding method, any change in the protective gas composition or its current rate must be such that it does not interrupt the protection [53, 54].

2.8 Review on conducted researches

In 2003, Joe et al. evaluated the impact toughness of bonding of Ti-6A1-4 V welded through GTAW. They prepared Charpy test specimens in such a way that impact toughness of three areas of base metal, the weld area and the area affected by heat could be compared with each other. Their research showed that microhardness of the weld area was higher than the area affected by heat and impact toughness of this area was also 50% higher than the two other areas. They attributed the improvement of impact toughness to reduction in the initial alpha grains in the weld area. Grain boundaries of initial alpha are considered the preferred placed for germination of microcracks and provide easy routs for crack propagations [19].

In a research in 2008, Balasubramanian et al., with the aim of predicting the tensile properties of welded Ti-6Al-4 V, applied mathematical modeling of the pulsed current technique. This modeling was done by taking into account 4 variables in 5 levels of change and designing the test by response surface methodology. The efficiency of the model was verified using analysis of variance (ANOVA table). They provided an efficient model with a confidence level of 99% to predict the obtained weld tensile properties [33].

In another research in 2011, Balasubramanian et al. evaluated the growth of fatigue cracks of Ti-6Al-4 V welded through TIG method, electron beam and laser beam. They observed the highest and the lowest growth resistance of fatigue crack in the made weld, respectively, through laser beam method and TIG method. In addition, the growth resistance of fatigue crack was reduced after welding on this alloy. They attributed increase in growth resistance of the made weld though laser beam method to fine layer microstructure in the weld metal caused by lower input heat and higher cooling rate [34].

In the same year, Balasubramanian et al. examined the effect of type of welding method on the microstructure and mechanical properties of Ti-6Al-4 V welded through TIG, electron beam and laser beam. The weld strength made by electron beam welding was 6% and 2% higher than TIG and the laser beam. This is while the toughness of the weld made through TIG method was 35% higher than the other two methods due to presence of needle-shaped phases in grain boundaries and Widgetman Stroten's vaporization of α + β-biphasic area. They also reported the Vickers' hardness for TIG and electron beam welding, respectively, 403 and 509, and stated that by correcting the microstructure of the weld metal, it is possible to make changes in mechanical properties [55].

In 2011, Chen and Pan conducted a research using dynamic controlled plasma arc to minimize the heat input to a workpiece of Ti-6Al-4 V while maintaining full penetration.

They reported increase in toughness, hardness and ductility in the weld area due to reduction in beta-phase grain size, reduction in heat input and inhibition of making the hard martensitic phase in the penetrative area [10].

In 2015, Bohorquez and Cunha carried out a review study on ultrasonic methods in arc welding of alloys of titanium, steel and aluminum. They conclude improvement in the performance of arc welding processes at industrial scale using pulsed arc welding using the ultrasonic method, especially for alloys such as titanium alloys which have weldability problems [13].

In 2017, Singh et al. conducted a review study on methods for improving the penetration depth of weld in TIG welding of commercial pure titanium, aluminum and stainless steel. They focused on finding ways to eliminate defects in the low penetration depth of TIG welding and improving the mechanical properties of the resulted welds, and they knew use of flux (slag) or pulsed current effective to improve the penetration depth [14].

In 2017, Yang et al. welded the pulsed plasma arc of Ti-6Al-4 V. They reported a 24 to 30 percent decrease in grain size in the penetrative area, and 68 percent increase in the elongation quantity at frequency of 20 kHz, and a 38 percent increase in the elongation quantity at frequency of 40 kHz. In addition, in the end they introduced frequency range of 20–40 kHz as the best frequency range for the welding of this alloy [15].

2.9 Methods for evaluating properties of weld area

2.9.1 Metallography

In metallurgy, it is very important to observe, evaluate and determine the microstructure of phases or the components of the material, since it is possible to distinguish many properties of material and justify many of its behaviors under various conditions by microstructures. To achieve this, a metallographic method is used. Some uses of metallography is the awareness of the chemical composition and different properties of materials, detection of crystalline building, the history of mechanical work and the history of thermal operation carried out on the sample. To do a metallography, sample must be prepared first. The first step is to cut the piece that we want to prepare the sample of that. We use a cutter apparatus to cut the piece. This apparatus, while cutting, creates a coating of water on the piece because the collision of the cutter with the piece creates friction and increases the temperature of the cutting location during cutting, and if this temperature does not drop, the phase structure around the cutting location may change. To solve this problem, water is used up to decrease the temperature. Till now, the sample has been separated from the piece. In the next step, mounting muse be done. After preparing the mount, it is time for sanding; the sandpaper itself consists of 4 rows with numbers 240, 360, 600 and 1000. The sandpaper is soaked by water. The concept of 240 is that it has 240 holes (groove) per inch in square. First we use sandpaper 240. We select a specific direction on the sample and then sand toward that direction. By changing the sandpaper, this time, we will sand the sample in a perpendicular direction to the previous state. When all the lines are in one direction, we go to the next sandpaper. After sanding, we will thoroughly wash the sample with water. The next step is polishing, which uses a suspension (0.3 micron) of Al_2O_3. We pour it on a rotating disk fabric. To polish, one of the following three methods is used: we rotate the sample on the inverse rotation direction of the disk, or rotate it as shape of 8, or rotate it from side to middle of the disk, while moving it linearly, simultaneously. We do this 20 times each for 30 seconds. Then we wash the sample with water thoroughly. In the third step, we use 0.05 micron Al_2O_3 and a softer fabric on the disk. The pressure of the hand should be less than the previous step. When the sample lines disappear, we wash it with water and then alcohol. Then we dry it with a tissue paper and a heater. Now, we see the sample under a microscope. If there are many lines, we repeat one or more stages of the preparation process, depending on the number and depth of the lines, because these lines block the correct view of the sample, and sometimes lead to mistakes in conclusion and report of observations. The prepared sample does not show a particular image of the microstructure. To see the microstructure, we need to etch the sample (chemical engraving). Then we see the structure under the microscope [56–58].

2.9.2 Hardness

We consider hardness as a material resistance to plastic deformation. Although it is conceptually different to strength, but they both operate in the same direction. That is, if the hardness increases, strength increases and vice versa. The strength is a specific number but the hardness is relative. In the sense that the hardness of a material is measured relative to another. There are various definitions of hardness that vary depending on the application. These definitions are as follows:

- Resistance to penetration under static or dynamic forces
- Energy absorption under impact forces
- Scratch resistance
- Abrasion resistance
- Resistance to cutting of machining or drilling

There are different methods to get the hardness value. But in general, there are three general scale types of hardness: scratch hardness, hardness of return or reflection, penetration hardness. The technique of scratching is mostly used in mineralogy. The intended object is scratched with different materials. If the scratch does not occur, it shows that the object of is harder than the material used to scratch, and if not the opposite. This method is very old. Dynamic hardness test is a non-destructive method. A ball bearing is located inside a cylinder whose surfaces are burnished. The initial height of the ball bearing is specific. The cylinder is put on the surface that they want to test the hardness. The ball bearing falls and the hardness value of the material is measured based on the return height. The softer the matter, the more energy it absorbs, and therefore the lower the return height. The hardness in this case is as the unit of energy. Regarding the use of the third type of hardness test method, the types of hardness test are expressed against the penetrating object in following. In the hardness test method against the penetrating object, material resistance to a ball bearing or pyramid with specified dimensions and determined force is considered as hardness. The higher the resistance, the higher the handedness. This test is performed in different ways, which are categorized according to the type of penetrator and the applied pressure:

- Brinell

n this method, a steel ball bearing with 10 mm of diameter, 3000 kg of force for hard metals and up to 500 kg for soft metals are used. Also a tungsten carbide (WC) ball is used for hard metals. Usually, time of applying the force is between 20 and 30 seconds for iron alloys and 65 seconds for non-ferrous metals. The Brinell hardness number is expressed according to load on the internal area of the penetration. The advantage of using Brinell hardness test is that it is less susceptible to surface roughness and scratches than other hardness tests, and also the relatively large size of Brinell effect is useful in obtaining average local inhomogeneities. On the other hand, this large size of the effect can make it impossible to use this test for small pieces or pieces that are under critical stress and formation of penetration can cause fracture in them. Damage in this method is more than other methods.

- Meyer

In this method, instead of the area of the surface within the penetration, the effect surface is used. The average pressure between the penetrating surface and penetration is equal to the force divided by the effect surface. Meyer considered this mean pressure as the hardness, which is a more reasonable value than Meyer hardness.

- Vickers

In the Vickers hardness test, a square-base pyramid is used. The angle between the dimensions is 136 degrees. The reason for choosing this angle is that it is the best ratio of penetration diameter to the ball diameter in Brinell test. Due to penetrating shape, this test also known as the Diamond-Pyramid hardness test. The Diamond Pyramid Hardness Number (DPH) or the Vickers Hardness Number (VH or VHN) is obtained by dividing the force into the penetration area from the following equations:

$$VHN = \frac{2PSin\left(\frac{\theta}{2}\right)}{L^2} = \frac{1.854P}{L^2}$$

In the equation, L stands for average of diameters and P stands for the applied force. Vickers hardness test is acceptable for research works. Because it conducts a continuous test of hardness with a specific load from very soft metals with DPH equal to 5 to very hard materials with DPH equal to 1500. In this mode, the force varies from 1 to 1200 kilograms. Speed of this method is lower and is mostly used for hard materials. Error is also high in this method because error is high in measuring diameter of the effect. On the other hand, since in this hardness test the applied force does not depend on hardness of material so it is better than Brinell and Rockwell.

- Rockwell

In this hardness test method, a diamond-cone mandrel with a vertex angle of 120 degrees or a steel ball bearing of 1.16 or 1.8 inches is used. Since in this method the measurement error is low and speed of the action is high and the created effect is small, so it has many usages. At the beginning, a force equal to 10 kilograms is applied, which makes the surface need less readiness, and the tendency to create penetration or protuberance by mandrel. The application of this force also results in the loss of the oxide layer of the surface, which leads to better result, and then the main load will be applied. The hardness value in this case is given by the apparatus itself, and it is not necessary to measure the diameter of the effect and find the hardness number from the table [41, 59, 60]. In **Table 10**, the specifications of Rockwell Hardness Tests are presented.

2.9.3 Tensile test

One of the most important properties of material is resistance to normal tensile stress. When a piece is affected by tensile stress, it does undergo elastic deformation

Type of Rockwell	Type of Penetrator	Force (Kg)	Usage
A	Diamond-Cone	60	Cemented carbides. Steels that have been superficially hardened.
B	Steel ball bearing with diameter of 1.16	100	Alloys of copper and aluminum. Soft steels
C	Diamond cone	150	Steel-hard cast iron. Steels that have been deeply hardened
D	Diamond cone	100	Steels that have been moderately hardened and thin steels
E	Steel ball bearing with diameter of 1.8	100	Cast iron. Alloys of Al and Mg. Bearing metals
F	Steel ball bearing with diameter of 1.16	60	Annealed copper alloys
G	Steel ball bearing with diameter of 1.16	150	Phosphor bronze. Copper. Be. Malleable iron
H	Steel ball bearing with diameter of 1.8	60	Al. Pb. Zn

Table 10.
Specifications of Rockwell hardness tests.

until it reaches its elasticity, and stress and strain follow Hooke's law. The coefficient of this equation is called elastic modulus, which depends on the inherent conditions of materials. In the stress–strain diagram, the spot that shows the required stress to begin the plastic deformation, is called the elastic limit and the intended stress is called yield stress. Frangible materials get fracture after this stage, but other materials enter the plastic deformation stage. The increase in force continues as long as the effect of increasing the force is higher, due to hardness work, than effect of reducing the force due to reduction of the cross section, and when the two effects are equal, the force applied to the sample reaches its maximum value and at this point, the object starts to necking from the weakest point. Then increase of force continues until the material reaches a breakpoint and the stretch test is completed. To perform the tension test, the tensile test samples must first be prepared according to ASTM standards. The test consists of the following steps:

- To specify length of the gage on the sample. Length of the part that has the minimum diameter is called gage. Length, width and thickness of the gage are measured with the caliper.

- To place the gage part of the sample in the jaws of the apparatus, to proliferate the relative length and to decrease the cross-section.

- To set the initial status of the apparatus to zero and the speed of the jaws.

- To draw a curve of force variation in terms of length proliferation.

- To measure proliferation of the relative length and to reduce the cross-section after fracture of samples [41, 56, 59].

3. Experimental methodology

3.1 Research objective

Properties such as biocompatibility, corrosion resistance and a high strength ratio to weight have led to the use of titanium and its alloys, in spite of high prices in the pharmaceutical, petrochemical, aerospace industries. In many of these applications, the need for titanium jointing or their alloys is in a variety of ways. One of these jointing methods is welding. One of the most commonly used methods of titanium and its alloys welding is the arc-method of tungsten-neutral gas electrode. The variables of this process have a direct impact on the properties of the final product. Therefore, when welding of these alloys is required in different applications, the choice of welding variables should be achieved in such a way that the final microstructure and desired properties are obtained. In this welding process, variables such as current intensity, welding voltage, welding speed and protective gas have a significant effect on the final properties of the product. The purpose of this study is to investigate the impact of the input heat variety (welding current intensity) on the microstructure and mechanical properties of alloy-welded parts in Ti-6Al-4 V by arc-method of tungsten-neutral gas electrode. For this purpose, welding operation was done by selecting three current intensities of 80, 90 and 100 amperes and the results of the analyzes for these three current intensities were compared.

3.2 Laboratory facilities and raw materials

In this study, tungsten non-consumable Manual Metal, Ti-6Al-4 V sheets, argon-grid gas 6.0 as a protective gas and consumable and non-consumable welding wires of ER Ti.5 and EW Th.2 were used. The used welding machine was the manufacture of the Gam-Electric company, the 400 model. The work-piece was jointed to the positive pole and the electrode was jointed to the negative pole and the polarity of welding was DCEN.

3.3 Method of performing the research

On six sheets of 250 × 125 × 2 mm of Ti-6Al-4 V, three tests of PQR were used with welding process with non-consumable tungsten electrode with neutral gas protection with different welding variables. Then, the samples were joined by GTAW welding method by Square Joint with a number of welds. The welding operation at the first stage was performed at a current intensify of 30 amps, but the weld did not penetrate completely back of the sample and the test failed. At the next stage, in order to achieve full penetration, the sample joint model was changed from Square Joint to V shape, and the back-weld was used to protect the molten pool on back strain gas. In this case, the current intensity increased to 50 amps, and again, no full weld penetration was achieved after welding operation. At the last stage, the current intensity increased to 80A according to the above method, and in this case, full penetration was achieved. PQR test were taken with the current intensity of 90 and 100 amps in the second and third joint samples, and, as in the first case, a full penetration was

Current intensity	**80 amps and 90 and 100**
Voltage range	11–13
Joint model	V shape
Groove Angle	60 degree
Current Rate	Lit/min 25
Consuming Gas	Argon with a purity of 99/9999%
Tungsten Metal diameter	6 mm/1
Welding Wire Diameter	1 mm
Type of welding wire and consumable and non-consumable Welding speeds	ER Ti-5 و EW Th-2
Welding speeds	cm/sec 0.22 (for 80 amps current intensity) cm/sec 0.263 (for 90 amps current intensity) cm/sec 0.33 (for 100 amps current intensity)
Root Opening	mm 0–1
weld Bead	5–7 mm
Number of weld layers	1 layer
N/A	Pre-heat
N/A	PWHT
Gas current rate	12 lit/min

Table 11.
Specifications and variables of the performed welding processes.

obtained. It should be noted that all tests were performed according to ASME Section IX standard.

Table 11 shows the variables and Specifications of the performed welding operations. Also, the images of the performed welding operations have been in **Figure 9**.

3.4 Study methods and evaluating the properties

After the welding operation, the welding joint site was investigated using an optical microscope after metallography, so that the impact of changing the current intensity is investigated on the resulting microstructure and also their comparison is conducted with each other and with the base metal. In order to investigate the mechanical properties, samples were sent to Razi Foundation for Applied Sciences Laboratory for tests of

- Tensile,
- Impact and
- Hardness and Metallography

Figure 9.
Images of performed welding operations.

By the center.

In the next chapter, we will present the results of these experiments and will analyze and review them, and these results will be compared with the results of other studies.

4. Results & discussions

4.1 Introduction

This section has analyzed the data and the obtained results from the experiments. As it was already stated, these experiments have been performed on Ti-6Al-4 V. Three different electrical current intensities (welding amps) have been used to conduct experiments that included 80.90 and 100 amps, and the impact of the electric current intensity on the welding specifications has been studied. For this purpose, the weld hardness, and as well as the tensile strength of the samples have been studied and compared with the base electrode samples. In addition, the gained microstructure of the weld has been evaluated and studied in different welding areas and its different phases have been analyzed. In this chapter, the impact of electrical current has been analyzed on mechanical properties. Elongation increase:

Elongation increase has been measured also in this experiment. Elongation increase least rate has been related to the samples that have been jointed with the least current rate (80 amps) and it has been about 30% less than those that have been jointed to each other with current s above 90 and 100 amps. Elongation increase expresses the flexibility in some degree and has an inverse relationship with the weld strength. Its reason for this can be attributed to the weld structure, so that in welds that have been welded with a current of 80 amps, the beta phase has been more precipitated in the welds boundary, which causes the weld flexibility to decrease and Elongation Increase also decreases (**Figure 10**).

4.2 Tensile test

One of the most important welding targets in metals is to create a higher strength, or at least equal to the base metal, which can withstand the forces applied to the sample. In all welds, an attempt is made to increase the strength of the weld above the base metal, and there be no break in the weld and adjacent area of the weld and the

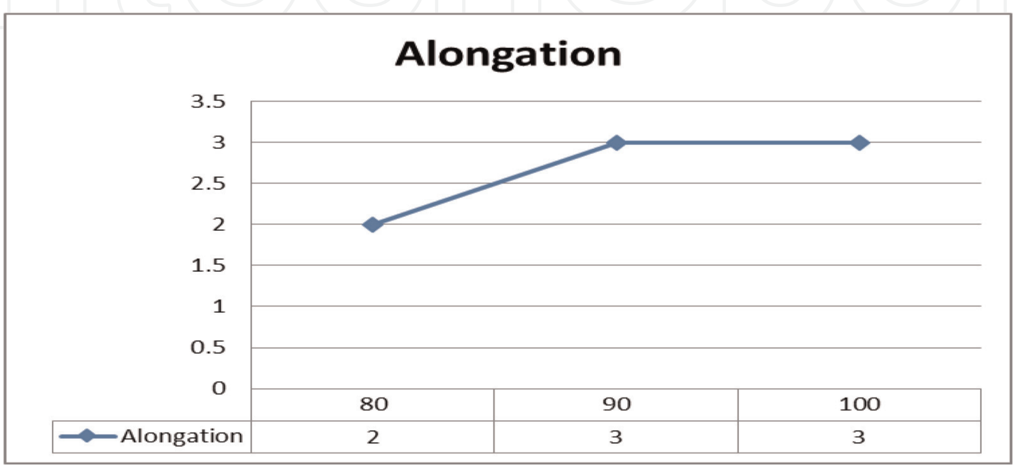

Figure 10.
Current effect on elongation increase.

break is made in the base metal. One of the most important tests for weld quality measurement is tensile test. In this test, the original sample and then other samples have been examined. Each sample has been tested three times for tensile test.

4.2.1 Yield strength

Yield strength for the measured samples is observable in the below figure. As it is known, the highest yield strength belongs to the current of 80 amps, due to the high percentage of beta phase, and as well as the impact of welds size (**Figure 11**).

By increasing the current rate, due to the change in the input heat rate to the weld area and also the change in the speed rate of the electrode, we observe that the yield strength decreases, so that with an increase in the current from 80 to 90 amps, we observe a 4% decrease in Yield Strength, and we will have a 21% decrease in strength by current increase to 100 amps (compared to 80 amps). In short, with welding current increase, we will observe a decrease in Yield Strength.

4.2.2 Ultimate strength

Ultimate Strength of the samples also has been measured also that has been shown in the below figure. As it is known, the highest Ultimate Strength belongs to the current of 80 amps and the lowest strength rate is also related to the current of 100 amps, which can be attributed to how the structure of the welds is changed, which the beta phase that is a needle-shape, it has been formed about 40% of the ground phase in the current of 80 amps, but in the current of 100 amps, about 30% of the ground phase is due to the needle-shape phase of the beta phase, this phase increases the ultimate strength of the weld, and during the 90 amps, 35% of the ground phase belongs to the beta phase. Also, the alpha phase, which somewhat reduces the strength, has the highest rate at 100 amps, with an approximate ratio of 70%, but within 80 Amps, only 60% of the phase forms the alpha phase. This structure change affects the ultimate strength of the weld (**Figures 12** and **13**).

Generally, the current increase to 100 amps has improved the welding conditions and has made it possible to achieve the lowest strength rate, which is above 1000 mega-Pascal, that it is because of the reduction of the input thermal energy to the weld area, due to the electrical current, which causes improvement of the localized melting

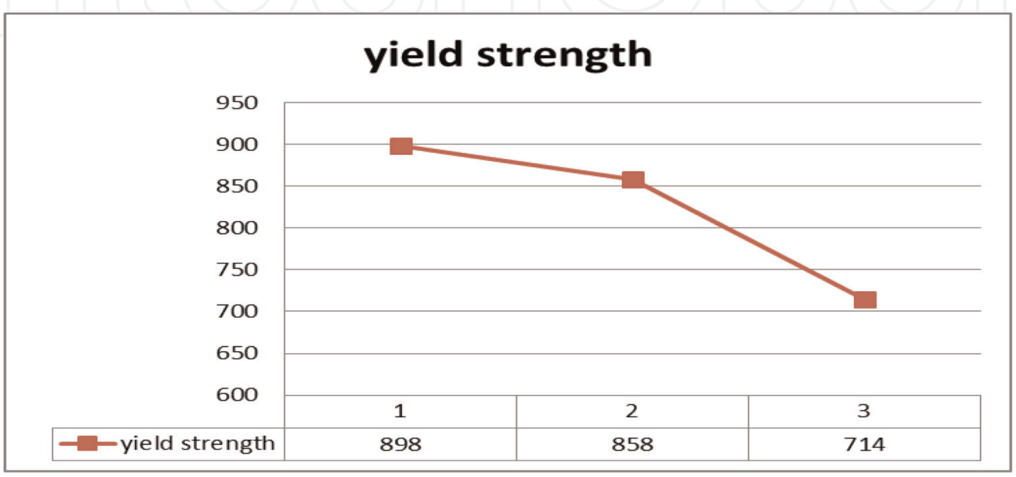

Figure 11.
Yield strength of samples that have been welded with electrical current intensities of 80, 90 and 100 amps.

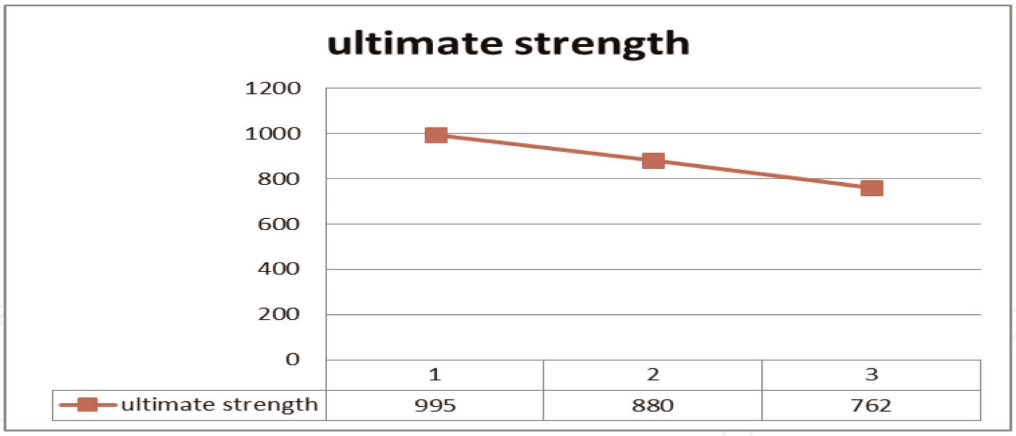

Figure 12.
Ultimate tensile strength of samples that have been welded with 80, 90 and 100 amps.

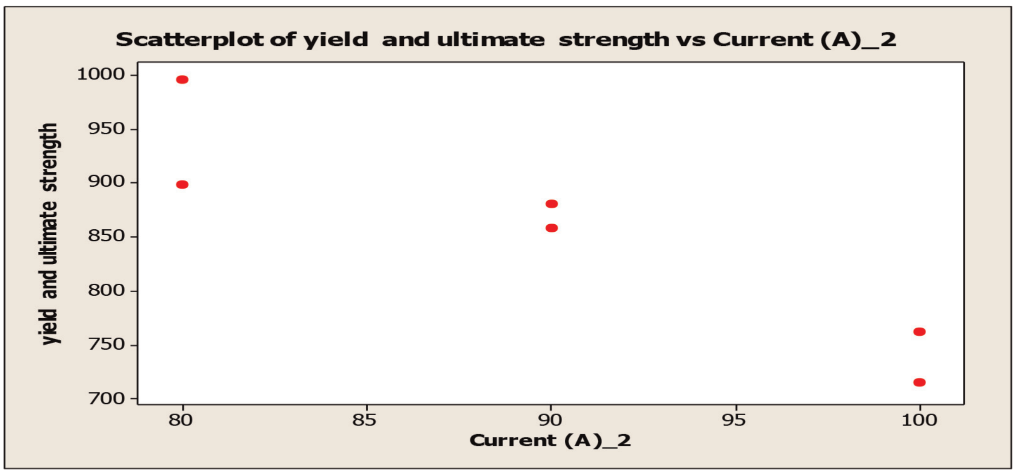

Figure 13.
Comparison of the ultimate strength and the tensile yield strength of the samples, which have been welded with electrical currents intensity at 80, 90 and 100 amps.

phenomenon and the melting of the two edges of the weld occurs better, which increases the flexibility of the welding.

In fact, the reason for increasing strength can be attributed to the weld microstructure, and the microscopic structure indicates that the weld area includes the alpha phase coarse-grain, and granular (bright) and the grain boundary phase of beta (dark). The beta phase stagnation in the alpha phase causes locking and the strength increase, but at a 100-amps the needle density (beta phase in alpha), the current ratio of 80 and 90 amps has been lower, which causes the strength of these samples reduces in comparison to two samples. The transformation of the base metal needle-shape structure (which increases the strength), into a coarse-weld structure is the main factor in affecting the mechanical specifications.

4.2.3 Micro-hardness

Vickers Micro-hardness test has been used to measure the hardness of the samples. Hardness test results show that increasing the electrical current reduces the weld hardness. As the electrical current increase causes the temperature increase and because of that the gradient beta phase has been decreased and the mechanical properties of the samples have been changed and the mechanical specifications of the samples have been changed and the increase of the electrical current causes the fine-weld structure in the weld area, which increases the hardness of the material.

However, the three samples tested showed different harnesses, but this hardness was tolerable in a reasonable range, so that the difference is less than 2% of the average hardness of the samples, due to the lack of uniformity of the phases.

4.2.4 Hardness test (Vickers) for current of 80 amps

Measuring samples that have been welded with a current of 80 amps, show that they have a higher hardness than the original metal sample (**Figure 14**).

4.2.5 Hardness test (Vickers) for current of 90 amps

The reason for the low hardness of samples that have been welded with a current of 90 amps can be attributed to the microstructure of the samples. In the current of 90 amps, we observe a coarse-grained structure that this coarse-grained structure reduces the hardness. The least difficulty related to the heat affected area, which is due to the effect of the annealing heat, due to the process which makes the area soften. In fact, the input heat rate in the affected area increases the grain size, resulting in the strength reduction and ultimately, the hardness reduces too (**Figure 15**).

4.2.6 Hardness test (Vickers) for 100 amps

The hardness of the samples have been welded at 100A has been measured and shows that these samples have a higher hardness than the base metal (**Figure 16**).

In this test, with increasing the current to 80 amps, we see an increase in the weld hardness, but the hardness decreases during 90 amps and eventually the hardness increases to reach the highest level by increasing the current to 100 amps (**Figure 17**).

The size and morphology of these grains depend on the heat transfer during freezing. The first determinant of grain size is the weld input heat. In this way, the grain size will be larger if using higher output heat. The mechanical properties of the melting area of titanium, depend on how the phase state changes during cooling in the phase stability temperature range, in addition to the initial grain size. The ultimate microstructure depends on the cooling speed above the state change temperature, which itself is a function of the welding process type, process parameters, and other welding conditions, such as the geometric shape of the piece and the method of

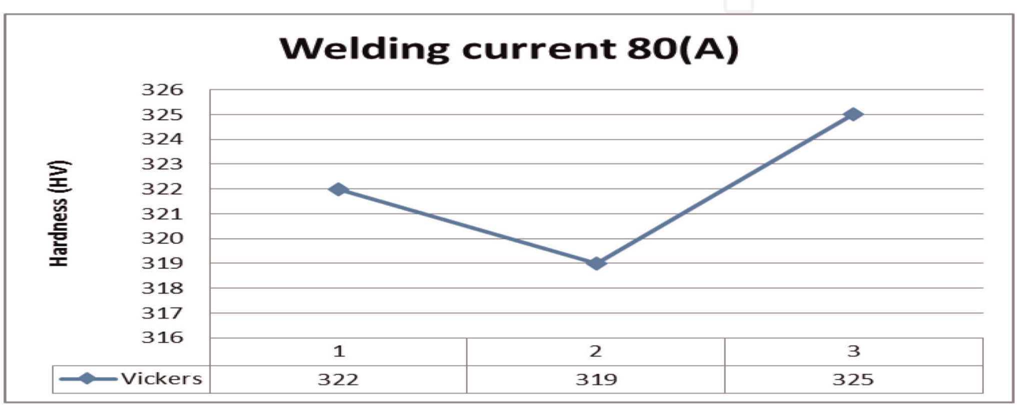

Figure 14.
Comparison of the hardness of the samples that have been jointed with the electrical current intensity of 80 amps.

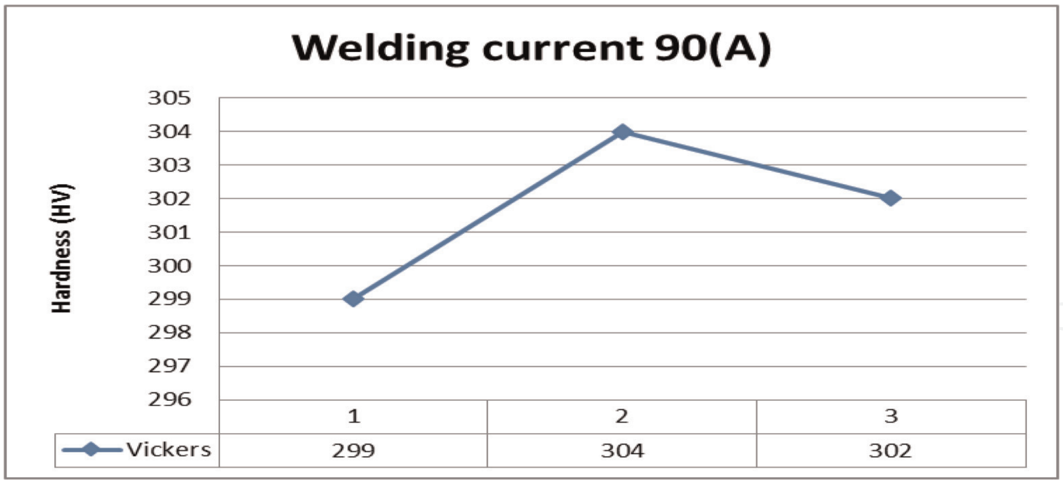

Figure 15.
Comparison of the hardness of the samples which have been jointed with the electrical current intensity of 90 amps.

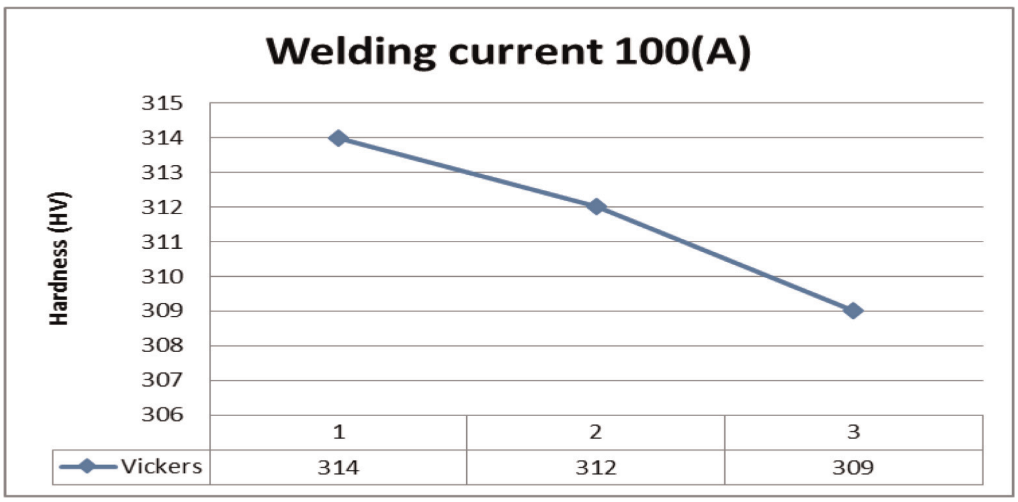

Figure 16.
Comparison of the hardness of the samples which have been jointed with the electrical current intensity of 100amps.

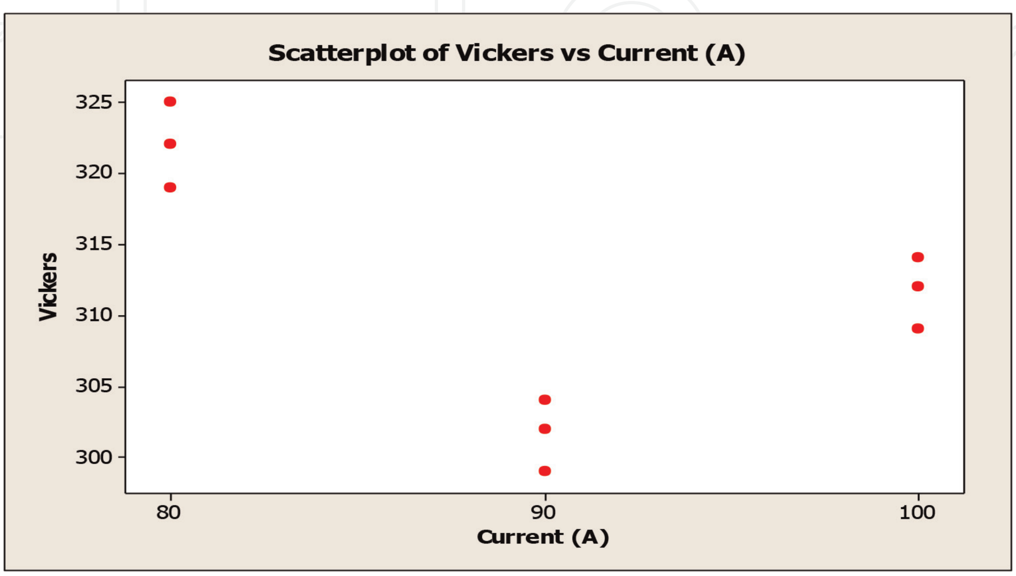

Figure 17.
Comparison of the hardness of samples that have been jointed with different electrical current.

fastening the piece. The microstructure is very fine and needle-shape, and its mechanical properties are strength and hardness versus low flexibility. The microscopic structure indicates that the weld area includes the alpha phase coarse-grain, and granular (bright) and the grain boundary phase of beta (dark). The formation of a base metal needle-shape structure that causes increasing the hardness to the base metal, and as well as coarseness of grains, is also responsible for affecting on mechanical properties such as hardness. However, in 100 A, the needle density (beta phase in alpha) has been lower than 80 and 90 A, which causes the reduction of the hardness of these samples than the other two. The formation of a base metal needle-shape structure, which causes the increase of the hardness to the base metal, and as well as coarseness of grains, is also a factor in affecting on the mechanical properties such as hardness.

4.2.7 Impact test: Charpy test

One of the tests that indicates the toughness of the material is the impact test. This test shows the weld energy level. One of the characteristics of titanium is toughness and malleability, which makes it absorb the energy of the hits and the forces and is not broken like a cast iron and Regarding that a good weld should be like the base metal, that does not cause a change in the structure and mechanical properties, so a good weld should also retain the toughness. The results of Charpy test for 80, 90, and 100 amps indicate that the toughness of the weld increases, by the electrical current increase and more energy is in need to break the weld. Titanium alloys contain one or more phase stabilizing elements, and their welding can effectively change the strength, flexibility and toughness of the weld-metal and the adjacent area of the weld. Usually, if these alloys contain more than 20% of the beta phase, their weldability is considered to be weak. Titanium beta alloys contain sufficient amounts of beta phase stabilizing elements.

This group of titanium alloys can be welded, but those beta-type titanium alloys that contain high amounts of phase-stabilizing elements have poor weldability because the welding metal has a high tensile strength. The mechanical properties of the welding zone, including the toughness of the titanium alloys, depend on the microstructures of FZ and HAZ areas, where the results of the Charpy test for 80, 90 and 100 amps indicate that with increasing electric current, the toughness of the welding increases and more energy is needed to break the weld, that its reason can be attributed to the change in the alpha and beta phases.

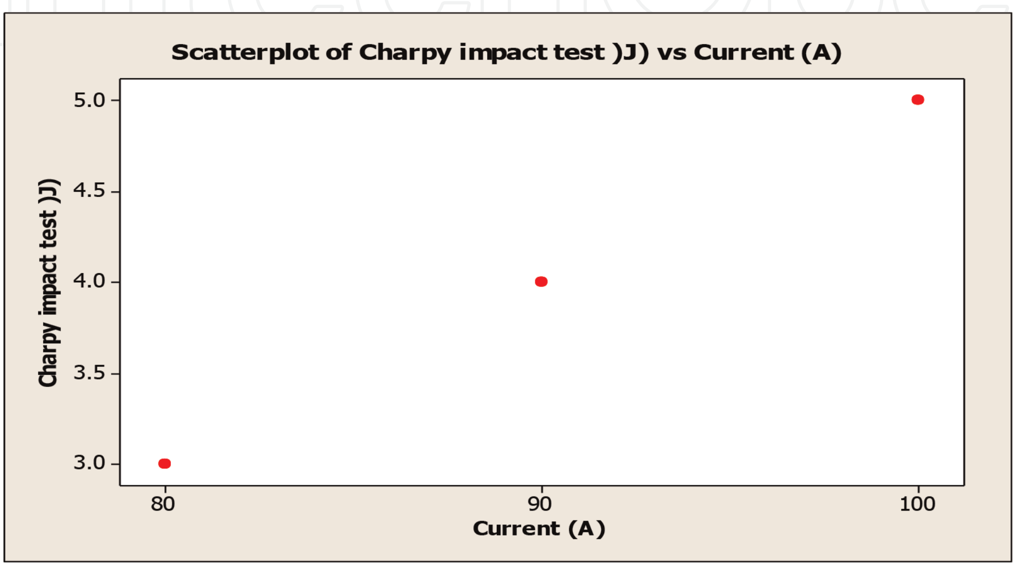

4.2.8 Welding section

The weld cross-section is semi-elliptic (pelvis-like), in which three distinct areas can be identified. Base metal area, weld area (pelvis-like) and heat affected area (**Figure 18**).

The area of the welded area and the heat affected area are directly affected by the welding parameters, and the welding parameters make this area smaller or larger. It is more appropriate that the welding area be smaller to give a good look to the piece and it will be suitable if the strength is appropriate.

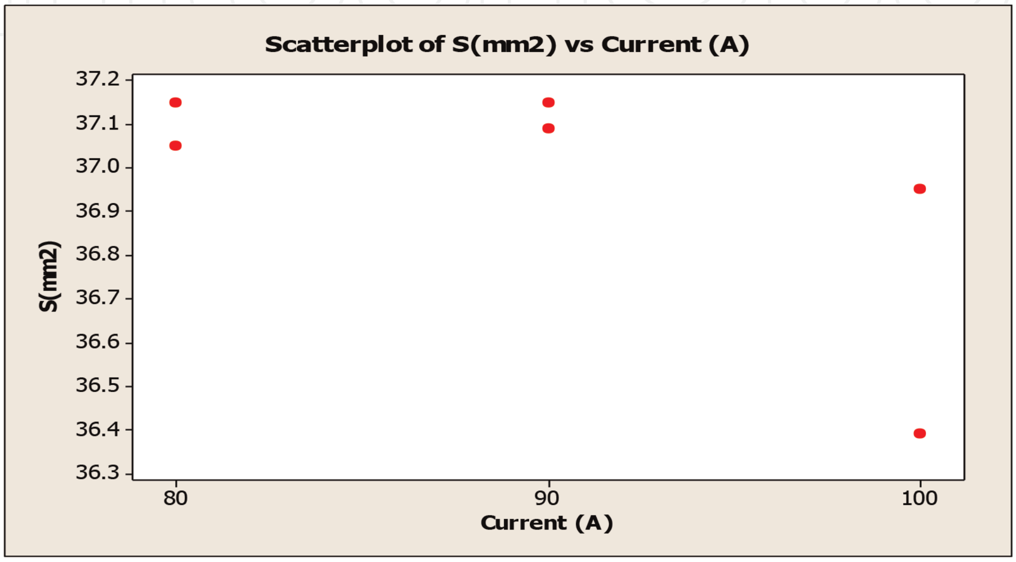

The area of the welded area and the heat affected area directly are affected by the welding parameters. The expansion of the weld area to the end of the metal will have a great effect on the quality and strength of the weld. For better examination, the weld is cut transversely, so that the cross-section can be clearly seen. In samples have been welded with less than 60 amps electrical current, it is clear that the lower area of the pieces is not well welded to each other, due to the lack of penetration of the tool into the lower part of the pieces, which it caused the pieces have not been fully jointed. The low electric current has been caused the metal in the two lower parts of the screen cannot be well-drained, which this will reduce the ultimate strength of the weld. The

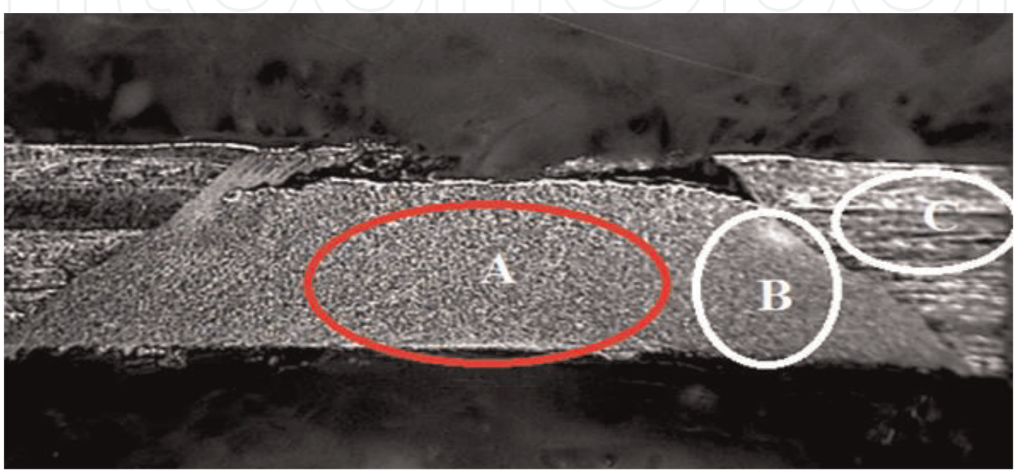

Figure 18.
Different areas of welding a: Welding area and mixing B: Heat affected area C: Base metal.

higher the electrical current, more heat will be produced, therefore the area of these two areas extends.

4.3 Metallography

For metallography of the weld samples, first they have been cut transversal, and the cut surface has been polished by the polish machine. Standardization of metallography has been carried out using ASTM E3–11 standard. After polishing the samples, using the etching process, samples have been prepared to see below under the microscope. For this purpose, the etching process has been used according to ASTM E407–2015 standard. Kroll solution has been used to visualize it. Also the process of optical microscopy has been performed according to ASTM E883–11 standard. Microscopic structure in base metal includes the alpha phase coarse-grain, and granular (bright) and the grain boundary phase of beta (dark).

4.3.1 Microstructure in base phase

The structure of the base metal is more regular and fine grain. In all samples, the alpha phase has been dominant, and the beta phase is observed only in the grain boundary (**Figure 19**).

Microstructure in the weld area includes the alpha phase fine-grain, and granular (bright) and the grain boundary phase of beta (dark).

4.3.2 Microscopic structure in the weld area

The fine grain structure in the weld area affects both the hardness and the tensile strength in accordance with Hall's hypothesis. It shows the microstructure of the affected area by heat, which is the same coarse-grain and needle-like jagged microstructure. Partial melted grains in the common solid-molten area are suitable sites for solid phase growth into the molten pools. The grains are increased in as the surface from the common solid-molten area to the weld line-center. Because the mechanical properties of the weld, especially its flexibility, depend on the grain size (**Figure 20**).

4.3.3 Microstructure due to weld

The following figure shows that the microstructure of the weld area is fine-grained, needle-shape and jagged. Titanium at medium temperature and pressure has

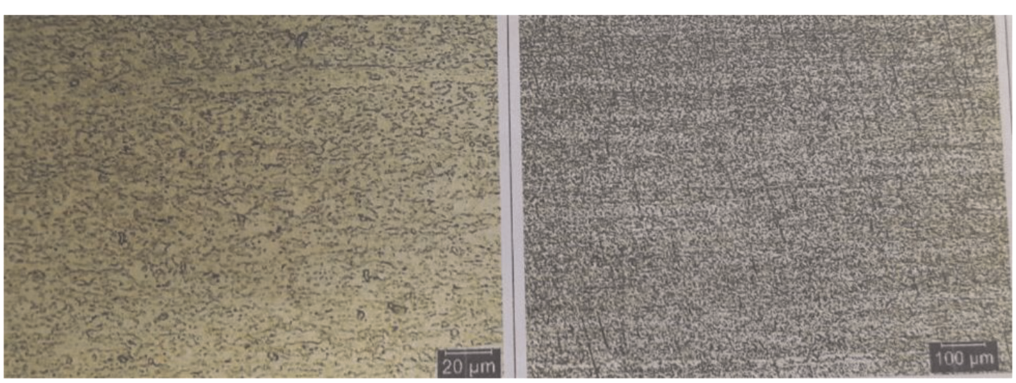

Figure 19.
Basic metal microstructure with two magnifications for 80 amps.

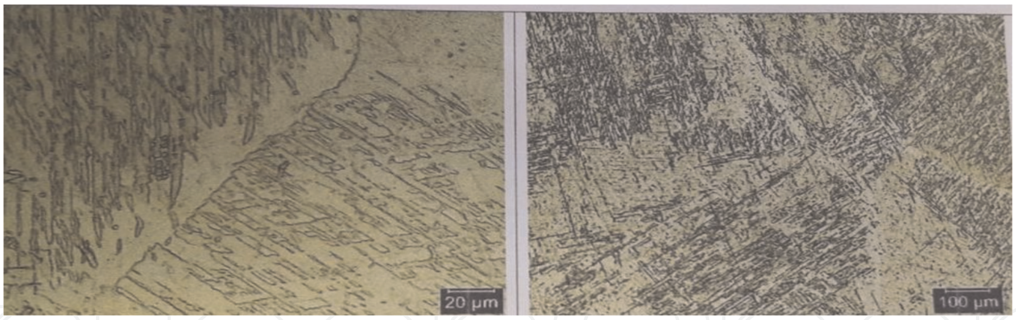

Figure 20.
The microstructure of the heat affected area with two magnifications for 80 amps.

a HCP crystalline structure with a compression ratio of (c/a) 1.587 (α phase). At 890 degree, Titanium is transformed into a β-phase with the crystalline BCC structure by the allotropic transformation, which this structure remains stable until the melting point (1678 degree). An increase in the electrical current increases the temperature during the process, which due to that, beta grain boundary phase has begun to grow and is increasing, and this increase in the beta phase in the weld area is higher than the heat affected area, due to the higher thermal gradient. Another factor influencing the beta phase increase is the cooling rate, which is highly dependent on the linear speed of the tool and the rotational speed of the tool has a minor effect, but it also can be ignored the effect of the cooling rate on the grain size of the beta phase and its amount, due to the linear speed constant in the disorder friction welding process of all five samples (**Figure 21**).

4.4 Material microstructure evaluation

During the welding operation, the microstructure of the weld area and the affected areas by it change, so evaluating these changes can help you understand the effects of the parameters on the mechanical and physical properties of the weld. For this purpose, the samples have been metallographed and then have been examined by optical microscopy. First, the microstructure of the base metal has been evaluated. The two phases of alpha and beta are the main phases of this alloy that can be clearly seen. The bright areas are related to the alpha phase, and the dark areas are also related to the beta phase (it should be noted that these two phases consist of two different crystalline structures). As it is evident in the figure, these two phases are completely

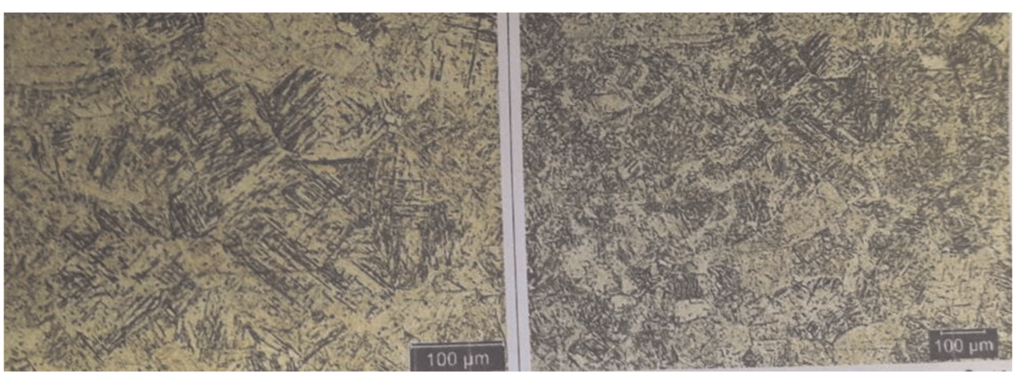

Figure 21.
Welded area microstructure with two magnifications for 80 amps.

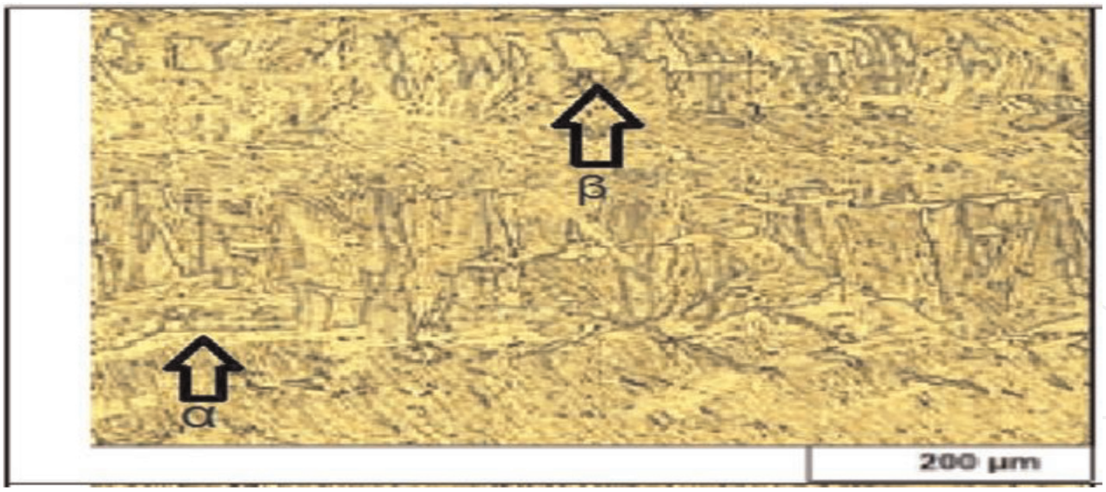

Figure 22.
Base material microstructure.

dispersed in each other, and the dominant phase is the alpha phase that the beta phase has been dispersed inside it (**Figure 22**).

4.5 Heat affected area

One of the areas that greatly affects the quality of the weld is the area affected by heat, which the microstructure of the area specifies the site and the type of weld break. The cold and stronger area around the weld area resists against the form that makes the affected area by thermo-mechanical operation. The specifications of the made form change in this area may also be covered by subsequent fuzzy transformations due to thermal cycles occurring during the process. Microscopic images show that the structure of the base metal, which is coarse-grain, has been turned into a more fine grain structure (of course relatively) in the heat affected area. Of course, this effect is less visible in samples that have been jointed in a low current. For example, in samples that have been jointed in 80 amps, also it is seen the structure of the alpha field along with the beta phase and is similar to the main metal, and this structure is more similar to the base metal, but we see the grains coarser and decrease of the beta6phase with an increase in the intensity of the current to 90 amps and clearly coarseness of grains is visible in 100 amps (**Figure 23**).

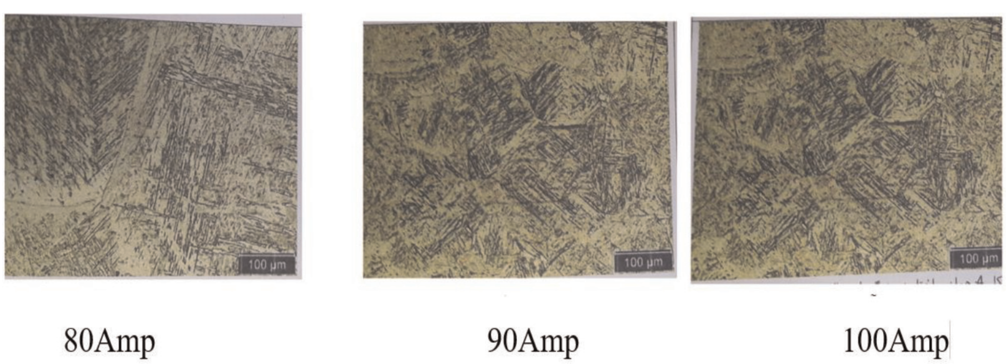

Figure 23.
Heat affected area microstructure in three different samples: A(80 Amp), B(90 Amp), C(100 Amp).

4.6 Weld area

Weld area is the most important Weld area that determines the quality of the weld. All the intermixing and thermo-dynamic phenomena happen in this part, so the microstructure of this area is very important. The special specifications of Titanium weld area are the presence of coarse grains during solidification of the weld metal in the molten pool area, resulting in a sharp decrease of its flexibility. The microstructure have been jointed in the samples with the least electrical current that they show the needle structure of the base metal has been converted into the coarse-grained structure in the samples, and as the electrical current increases, the size of the grains is also increased, so that the size of the grain in the metal weld area which has been jointed to with 100 amps is greater than the size of the grain of the weld area which has been jointed with 80 amps and the density of the needle-shape of the samples has been also increased.

This increase in density of the needle-shape (the placement of the beta phase in the alpha phase) affects the mechanical properties of the samples, which has been increased the strength of the samples compared to the base metal samples. The transformation of the needle-shape structure of the base metal (which increases the strength), into a coarse-grained structure is the main factor in effect on the mechanical properties. In fact, in the low currents, the made heat softens the weld (**Figure 24**).

The weld structure in samples that have been jointed with high-current shows that these structures contain a large number of needle-shape grains, which this is far more than the base metal.

Needle-shape grains behave like dislocation and prevent the movement of the material in the tensile test process and cause the weld strength increases compared to the main metal and break does not occur in the weld area. This mode is an ideal weld. But the interesting point is being needle-like density in a sample has been welded with 90 A, which being needle-shape density was reduced with 80 A and 100 A, which reduces its mechanical properties, which is also confirmed by tensile and hardness tests.

In the molten welding, titanium alloys, non-alloy titanium and alpha titanium alloys have a good weldability. That is, there is no significant difference in terms of microstructure and mechanical properties between the weld areas, the adjacent to the weld area and the base metal, and the resulting weld has sufficient strength with suitable flexibility.

4.7 Experiment results

4.7.1 *Effect of electric current on the weld hardness*

The results of the experiments show that the hardness of the base metal is always more than the hardness of the weld, which can be attributed to the softening and

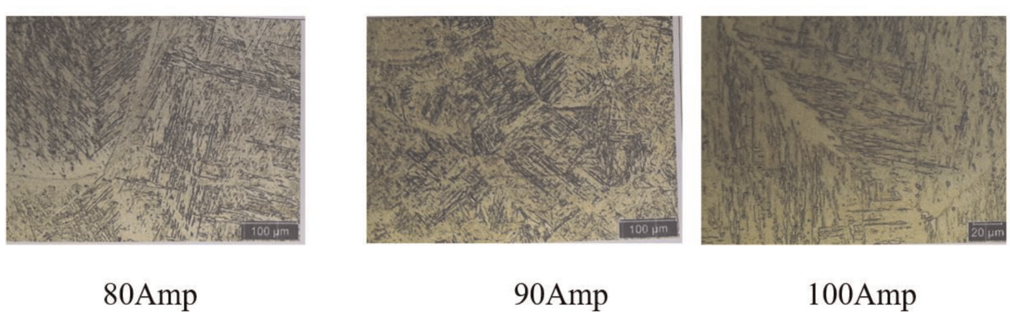

Figure 24.
Weld area microstructure in three different samples: A(80 Amp), B(90 Amp), C(100 Amp).

coarse structure of the metal in the weld area, where the output heat only results in the coarse-grain of the weld area and, as a result, increased hardness. Of course, with increasing the rate of electrical current from 80 amps to 100 amps, we will face the reduction of the hardness, because the intensity increase in the electrical current will reduce the heat to the welded area and the intermetallic compounds will not be formed that will affect the hardness. Therefore, it can be expected that by increasing the electrical current above this rate, we can observe the reduction of the hardness of the weld above the base metal. It should be noted, however, that during 90 amps, the hardness decreases that can be related to the alpha phase intensity and the beta phase.

4.7.2 Effect of electrical current intensity on strength

Samples have been tested by tensile test to obtain the tensile strength of the samples to investigate the effect of electrical current intensity on the weld quality. The results of the experiments show that samples that have been welded with a current rate of 80 and 90 amps have a higher strength than the base metal and break does not occur in the weld. Of course, the samples that have been welded with an electrical current of 100 amps have a lower strength than the two previous samples, but this experiment showed that the lower level of the electrical current rate that causes the weld does not have the required quality is below 80 amps (according to other parameters of this experiment).

4.7.3 Effect of welding current intensity on microstructure

Microscopic results show that the structure of the base metal consists of coarse-grained alpha-beta phases that have been interpenetrated in needle-shape form, which this structure is converted to a coarse-grain structure with a needle-shape low density in high electrical current intensity in the weld area, which is one of the main reasons for reducing the weld strength which causes no barrier (grain boundary) against material flux and consequently reduces the strength of the material, so that in samples that have been jointed with higher electrical current, we observe the lower hardness and strength.

4.7.4 Offers

Considering the great capabilities of titanium welding and the gained experiences in this research, suggestions are suggested for improving this method:

1-Performing the process inside the neutral gas:

Due to the high impact of titanium on the environment and the possibility of entering nitrogen, hydrogen and oxygen gases into the weld pool, it is suggested that this process is also carried out in a vacuum environment to increase the weld quality.

Chapter four Appendices figures: (Welding Procedure Specification).

DOI: http://dx.doi.org/10.5772/intechopen.106677

A. Appendix

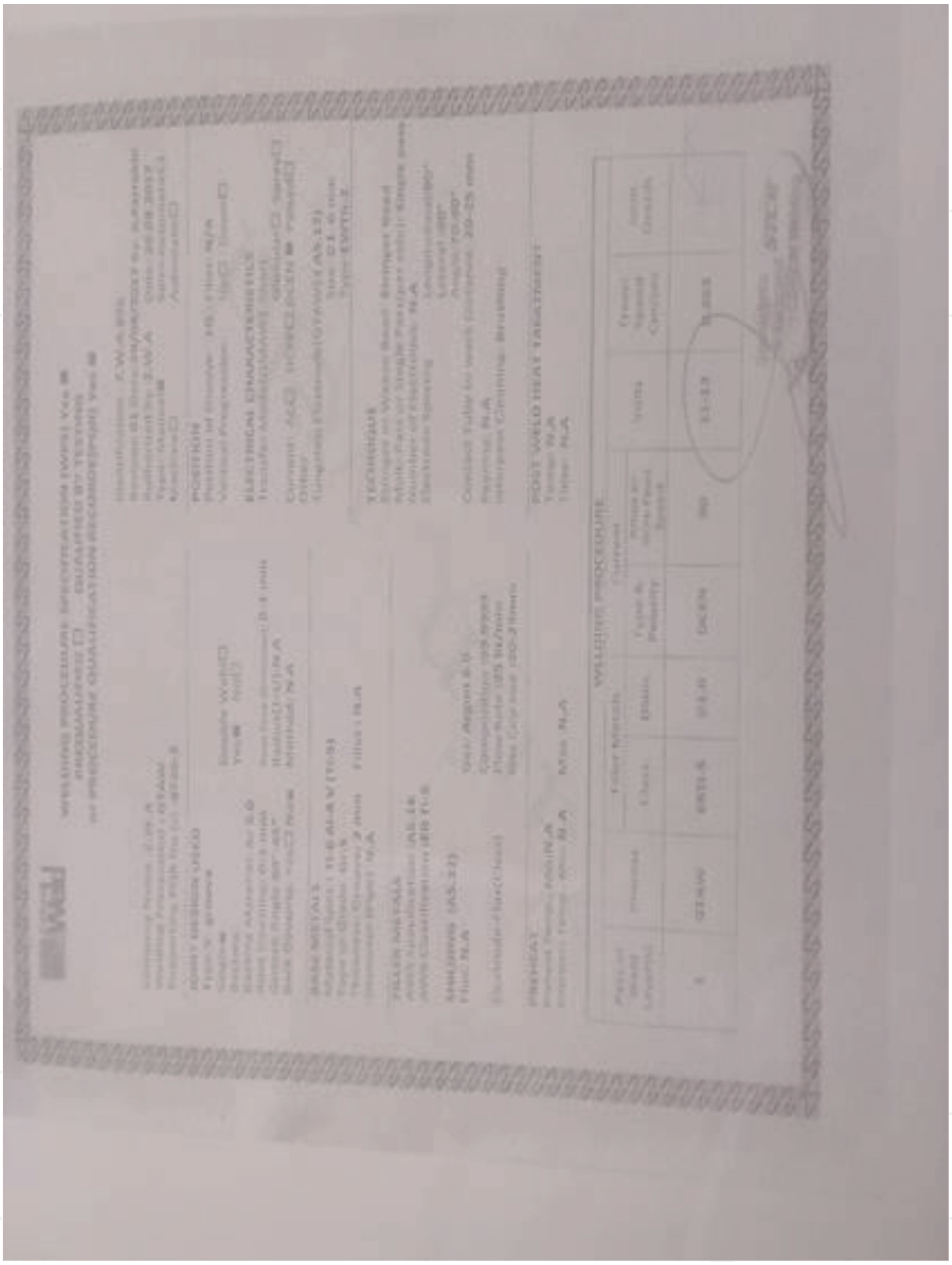

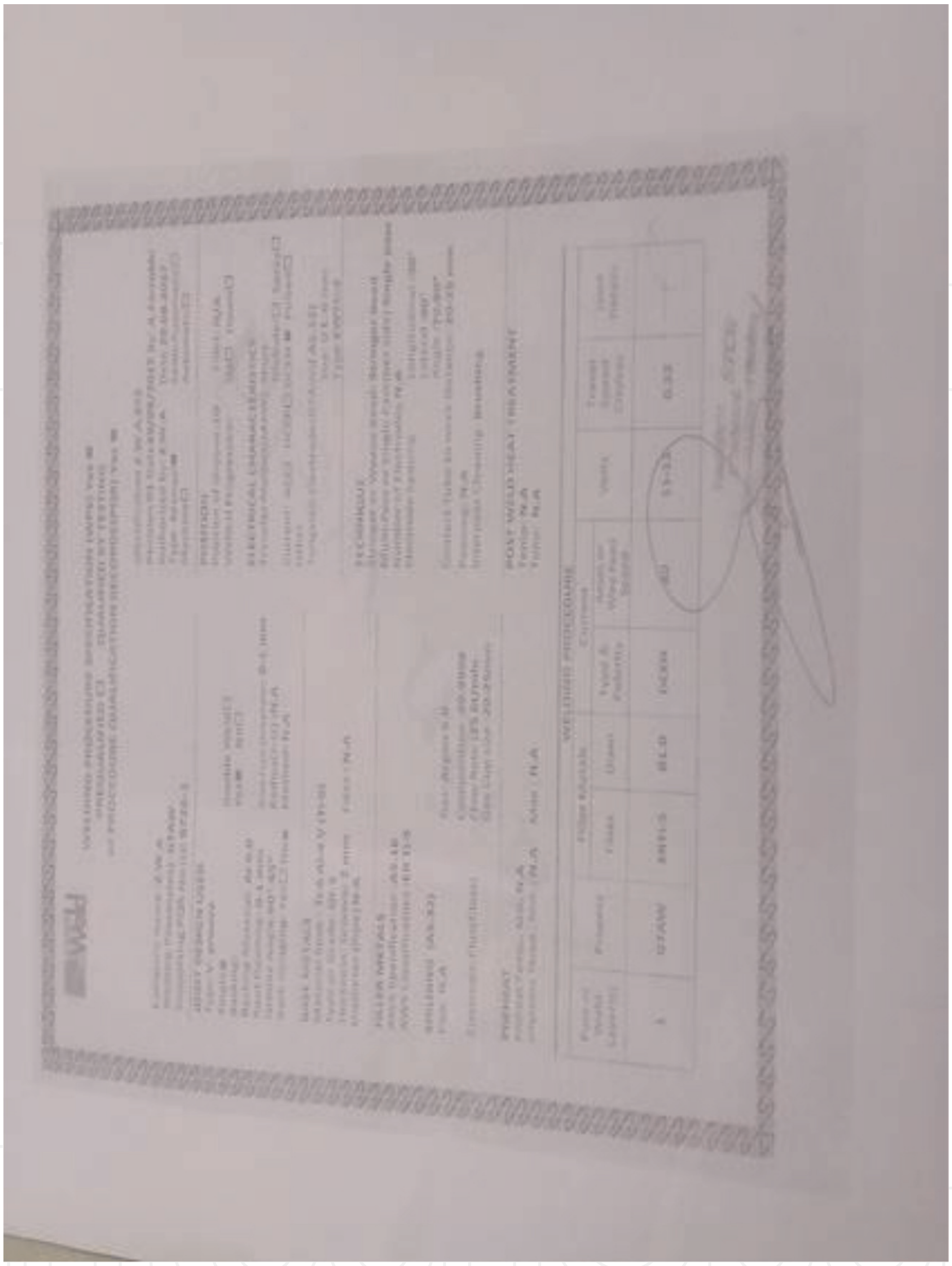

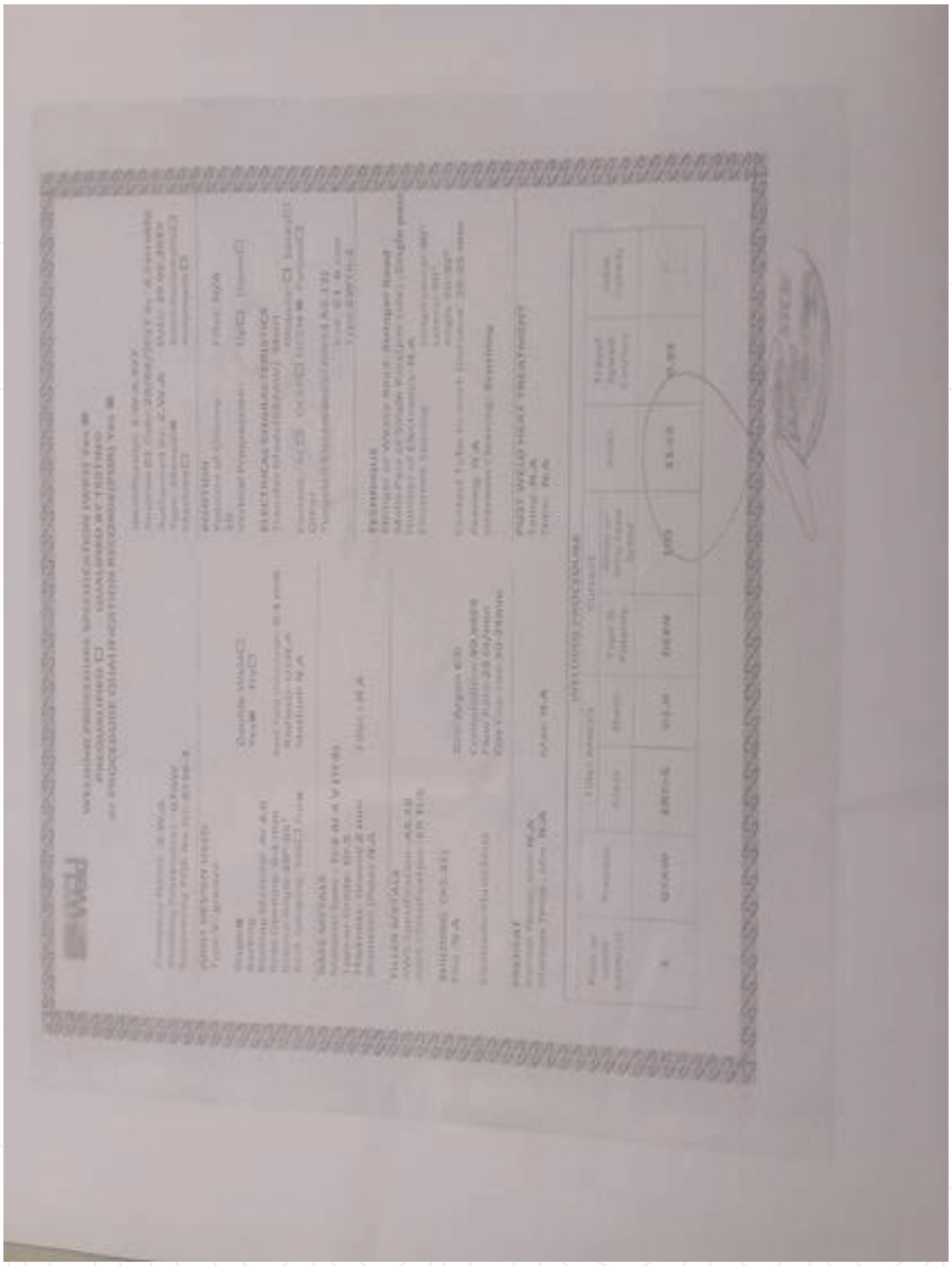

IntechOpen

IntechOpen

Author details

Alireza Farrokhi
National Valley University in California, USA

*Address all correspondence to: alifarrokhi5@gmail.com

IntechOpen

© 2022 The Author(s). Licensee IntechOpen. This chapter is distributed under the terms of the Creative Commons Attribution License (http://creativecommons.org/licenses/by/3.0), which permits unrestricted use, distribution, and reproduction in any medium, provided the original work is properly cited.

References

[1] Leyens C, Peters M, editors. Titanium and Titanium Alloys: Fundamentals and Applications. Germany: John Wiley & Sons; 2003

[2] Navedra Navedtra 14251 A Cost Comparison of welding processes.

[3] Boyer RR, Briggs RD. The use of β titanium alloys in the aerospace industry. Journal of Materials Engineering and Performance. 2005;**14**(6):681-685

[4] Lütjering G, Williams JC. Titanium. Berlin/Heidelberg , Germany: Springer Science & Business Media; 2007

[5] Welsch G, Boyer R, Collings EW, (Eds.). Materials Properties Handbook: Titanium Alloys. USA: ASM International; 1993

[6] Charles C. Microstructure Model for Ti-6Al-4V Used in Simulation of Additive Manufacturing [thesis]. Sweden: Luleå tekniska universitet; 2016

[7] Boyer RR. An overview on the use of titanium in the aerospace industry. Materials Science and Engineering: A. 1996;**213**(1–2):103-114

[8] Donachie MJ. Titanium: a technical guide. USA: ASM International; 2000

[9] Short AB. Gas tungsten arc welding of α+ β titanium alloys: A review. Materials Science and Technology. 2009;**25**(3): 309-324

[10] Chen JC, Pan CX. Welding of Ti-6Al-4V alloy using dynamically controlled plasma arc welding process. Transactions of Nonferrous Metals Society of China. 2011;**21**(7):1506-1512

[11] Niagaj J. Peculiarities of A-TIG welding of titanium and its alloys. Archives of Metallurgy and Materials. 2012;**57**(1):39-44

[12] Babu NK, Raman SGS. Influence of current pulsing on microstructure and mechanical properties of Ti–6Al–4V TIG weldments. Science and Technology of Welding and Joining. 2006;**11**(4):442-447

[13] da Cunha TV, Bohórquez CEN. Ultrasound in arc welding: A review. Ultrasonics. 2015;**56**:201-209

[14] Singh AK, Dey V, Rai RN. Techniques to improve weld penetration in TIG welding (a review). Materials Today: Proceedings. 2017;**4**(2):1252-1259

[15] Yang M, Zheng H, Qi B, Yang Z. Effect of arc behavior on Ti-6Al-4V welds during high frequency pulsed arc welding. Journal of Materials Processing Technology. 2017;**243**:9-15

[16] Kumar P, Datta CK. Pulsed parameters optimization of GTAW process for mechanical properties of Ti-6Al-4V alloy using Taguchi method. IJESIT. 2012;**1**(1):75-80

[17] Akbari M, Saedodin S, Toghraie D, Shoja-Razavi R, Kowsari F. Experimental and numerical investigation of temperature distribution and melt pool geometry during pulsed laser welding of Ti6Al4V alloy. Optics & Laser Technology. 2014;**59**:52-59

[18] Stenbacka N, Choquet I, Hurtig K. Review of arc efficiency values for gas tungsten arc welding. In: IIW Commission IV-XII-SG212, Intermediate Meeting, BAM, Berlin, Germany, 18–20 April, 2012. Berlin, Germany; 2012. pp. 1-21

[19] Zhou W, Chew KG. Effect of welding on impact toughness of butt-

joints in a titanium alloy. Materials Science and Engineering: A. 2003; **347**(1):180-185

[20] Tolvanen S. Microstructure and Mechanical Properties of Ti-6Al-4V Welds Produced with Different Processes [Thesis]. Sweden: Halmers University of Technology; 2016

[21] Taylor JC, Hondrum SO, Prasad A, Brodersend CA. Effects of joint configuration for the arc welding of cast Ti-6Al-4V alloy rods in argon. The Journal of Prosthetic Dentistry. 1998; **79**(3):291-297

[22] ASM International. Handbook Committee., ASM Handbook. Vol. 6a. USA: ASM International; 1993

[23] Weman K. Welding Processes Handbook. Sweden: Elsevier; 2011

[24] Leary RK, Merson E, Birmingham K, Harvey D, Brydson R. Microstructural and microtextural analysis of InterPulse GTCAW welds in Cp-Ti and Ti–6Al–4V. Materials Science and Engineering: A. 2010;**527**(29):7694-7705

[25] Wells ME, Richardson J. Recommendations and Requirements for Welding and Inspection of Titanium Piping for US Navy Surface Ship Applications (No. CARDIVNSWC-TR-61-98-18). Bethesda, MD: Naval Surface Warfare Center Carderock Division; 1999 Survivability Structures and Materials Directorate

[26] Khaled Z. An investigation of pore cracking in titanium welds. Journal of Materials Engineering and Performance. 1994;**3**(3):419-434

[27] Karimzadeh F, Salehi M, Saatchi A, Meratian M. Effect of microplasma arc welding process parameters on grain growth and porosity distribution of thin sheet Ti6Al4V alloy weldment. Materials and Manufacturing Processes. 2005; **20**(2):205-219

[28] Panwariya C. Evaluation of Nitride Layer on Ti-6Al-4V Titanium Alloy by Tungsten Inert Gas (TIG) Nitriding Method (thesis). Rourkela, Odisha: NIT; 2016

[29] Semiatin SL, Knisley SL, Fagin PN, Barker DR, Zhang F. Microstructure evolution during alpha-beta heat treatment of Ti-6Al-4V. Metallurgical and Materials Transactions A. 2003; **34**(10):2377-2386

[30] Ucok I, Kramer LS, Gungor MN, Wolfe P, Dong H, Tack WT. Effect of welding on microstructure and tensile properties of flowformed Ti-6Al-4V tubes. Materials Science and Engineering: A. 2005;**410**:160-164

[31] Radhakrishnan VM. Welding Technology and Design. New Dehli, India: New Age International; 2006

[32] Mehdi B, Badji R, Ji V, Allili B, Bradai D, Deschaux-Beaume F, et al. Microstructure and residual stresses in Ti-6Al-4V alloy pulsed and unpulsed TIG welds. Journal of Materials Processing Technology. 2016;**231**:441-448

[33] Balasubramanian M, Jayabalan V, Balasubramanian V. Developing mathematical models to predict tensile properties of pulsed current gas tungsten arc welded Ti–6Al–4V alloy. Materials & Design. 2008;**29**(1):92-97

[34] Balasubramanian TS, Balasubramanian V, Manickam MM. Fatigue crack growth behaviour of gas tungsten arc, electron beam and laser beam welded Ti–6Al–4V alloy. Materials & Design. 2011;**32**(8):4509-4520

[35] American Welding Society. Specification for Tungsten and Tungsten Alloy Electrodes for Arc Welding and Cutting. USA: ANSI-AWS A5.12M-98, February 1998

[36] American Welding Society. Filler Metal Procurement Guidelines. USA: ANSI/AWS A5.01–93; 1993

[37] Cary HB. Modern Welding Technology. USA: Prentice-Hall; 1979

[38] Albrecht AK. System Development for Analysis of Gas Tungsten Arc Welding [thesis]. USA: Vanderbilt University Institutional Repository; 2005

[39] Saitta Alexander M, Oates WR. Welding Handbook.: Materials and Applications. USA: American Welding Society; 1998

[40] Pires JN, Loureiro A, Bölmsjo G. Welding Robots: Technology, System Issues and Application. Portugal: Springer Science & Business Media; 2006

[41] Kou S. Welding metallurgy. New York, USA: John Wiley & Sons; 2003

[42] Nandagopal K, Kailasanathan C. Analysis of mechanical properties and optimization of gas tungsten arc welding (GTAW) parameters on dissimilar metal titanium (6Al 4V) and aluminium 7075 by Taguchi and ANOVA techniques. Journal of Alloys and Compounds. 2016; **682**:503-516

[43] Babu NK, Raman SGS, Mythili R, Saroja S. Correlation of microstructure with mechanical properties of TIG weldments of Ti–6Al–4V made with and without current pulsing. Materials Characterization. 2007;**58**(7):581-587

[44] Murthy KK, Potluri NB, Sundaresan S. Fusion zone microstructure and fatigue crack growth behaviour in Ti-6Al-4V alloy weldments. Materials Science and Technology. 1997; **13**(6):503-510

[45] Keshava Murthy K, Sundaresan S. Fracture toughness of Ti-6Al-4V after welding and postweld heat treatment. Welding Journal. 1997;**76**(2):81-s

[46] Mohandas T, Srinivas M, Kutumbarao VV. Effect of post-weld heat treatment on fracture toughness and fatigue crack growth behaviour of electron beam welds of a titanium (a+ b) alloy. Fatigue and Fracture of Engineering Materials and Structures. 2000;**23**(1):33-38

[47] Sundaresan S, Ram GJ, Reddy GM. Microstructural refinement of weld fusion zones in α–β titanium alloys using pulsed current welding. Materials Science and Engineering: A. 1999;**262**(1): 88-100

[48] Salama MM. Fatigue crack growth behavior of titanium alloy Ti-6Al-4V and weldment. TRANSACTIONS-AMERICAN SOCIETY OF MECHANICAL ENGINEERS JOURNAL OF OFFSHORE MECHANICS AND ARCTIC ENGINEERING. 2001;**123**(3): 141-146

[49] Atapour M, Fathi MH, Shamanian M. Corrosion behavior of Ti–6Al–4V alloy weldment in hydrochloric acid. Materials and Corrosion. 2012; **63**(2):134-139

[50] Yang Z, Qi B, Cong B, Liu F, Yang M. Microstructure, tensile properties of Ti-6Al-4V by ultra-high pulse frequency GTAW with low duty cycle. Journal of Materials Processing Technology. 2015;**243**:37-47

[51] Li QM, Wang XH, Zou ZD, Jun W. Effect of activating flux on arc shape and

arc voltage in tungsten inert gas welding. Transactions of Nonferrous Metals Society of China. 2007;**17**(3):486-490

[52] Zhang WJ, Liu YK, Wang X, Zhang YM. Characterization of three-dimensional weld pool surface in GTAW. Welding Journal. 2012;**91**(7): 195s-203s

[53] Onsoien M, Peters R, Olson DL, Liu S. Effect of hydrogen in an argon GTAW shielding gas: Characteristics and bead morphology. In: AWS 75th Annual Meeting, Held April 10–14, 1995. Philadelphia, PA; 1995

[54] Bitharas I, Campbell SW, Galloway AM, McPherson NA, Moore AJ. Visualisation of alternating shielding gas flow in GTAW. Materials & Design. 2016;**91**:424-431

[55] Balasubramanian TS, Balakrishnan M, Balasubramanian V, Manickam MM. Influence of welding processes on microstructure, tensile and impact properties of Ti-6Al-4V alloy joints. Transactions of Nonferrous Metals Society of China. 2011;**17**(6): 1253-1262

[56] Reed-Hill RE, Abbaschian R. Physical Metallurgy Principles. Monterey, Calif, USA: Brooks/Cole Engineering Division; 1973

[57] Raghavan V. Physical Metallurgy: Principles and Practice. New Delhi, India: PHI Learning Pvt. Ltd; 2015

[58] Pearson WB. A Handbook of Lattice Spacings and Structures of Metals and Alloys: International Series of Monographs on Metal Physics and Physical Metallurgy. Vol. 4. London, Paris, New York , Frankfurt: Elsevier; 2013

[59] Dieter GE, Bacon DJ. Mechanical Metallurgy. Vol. 3. New York: McGraw-hill; 1986

[60] Hertzberg RW. Deformation and Fracture Mechanics of Engineering Materials. Hoboken, New Jersey: Wiley; 1989

IntechOpen

IntechOpen